Science of the Total Environment 860 (2023) 160407

Contents lists available at ScienceDirect

Science of the Total Environment

journal homepage: www.elsevier.com/locate/scitotenv

Hotspots of geogenic arsenic and manganese contamination in groundwater of the floodplains in lowland Amazonia (South America)

Caroline M.C. de Meyer [a,*,1], Ingo Wahnfried [b], Juan M. Rodriguez Rodriguez [c], Rolf Kipfer [a,d], Pilar A. García Avelino [c], Edward A. Carpio Deza [c], Michael Berg [a,*]

[a] Eawag, Swiss Federal Institute of Aquatic Science and Technology, 8600 Dübendorf, Switzerland
[b] UFAM, Universidade Federal do Amazonas, Manaus, Brazil
[c] Facultad de Ciencias, Universidad Nacional de Ingeniería, Lima, Peru
[d] Institute of Biogeochemistry and Pollutant Dynamics and Institute of Geochemistry and Petrology, ETH Zurich, 8092 Zurich, Switzerland

HIGHLIGHTS

- Reconnaissance study of groundwater-chemistry of riverine areas in the Amazon Basin
- Basin-wide geogenic groundwater arsenic and manganese contamination documented
- Aquifers at risk of contamination delineated by fluvial geomorphology and topography
- Highest risk in the dynamic part of floodplains of sediment-rich rivers
- Reducing aquifer conditions in Amazonia comparable to floodplains in South and Southeast Asia

GRAPHICAL ABSTRACT

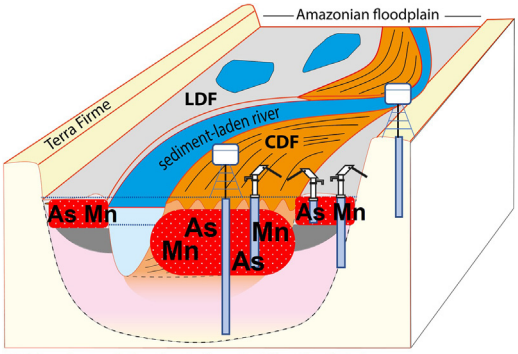

CDF = channel-dominated part of the floodplain
LDF = less dynamic part of the floodplain

ARTICLE INFO

Editor: Christian Herrera

Keywords:
Holocene aquifers
Amazon River
Hydrochemistry
Drinking water
Peru
Brazil

ABSTRACT

Arsenic enrichment in groundwater resources in deltas and floodplains of large sediment-rich rivers is a worldwide natural hazard to human health. High spatial variability of arsenic concentrations in affected river basins limits cost-effective mitigation strategies. Linking the chemical composition of groundwater with the topography and fluvial geomorphology is a promising approach for predicting arsenic pollution on a regional scale. Here we correlate the distribution of arsenic contaminated wells with the fluvial dynamics in the Amazon basin. Groundwater was sampled from tube wells along the Amazon River and its main tributaries in three distinct regions in Peru and Brazil. For each sample, the major and trace element concentrations were analyzed, and the position of the well within the sedimentary structure was determined. The results show that aquifers in poorly weathered sediments deposited by sediment-rich rivers are prone to mobilization and accumulation of aqueous arsenic and manganese, both in sub-Andean foreland basins, and in floodplains downstream. Two zones at risk are distinguished: aquifers in the channel-dominated part of the floodplain (CDF) and aquifers in the overbank deposits on the less-dynamic part of the floodplain (LDF). Some 70 % of the wells located on the CDF and 20 % on the LDF tap groundwater at concentrations exceeding the WHO guideline of 10 μg/L arsenic (max. 430 μg/L), and 70 % (CDF) and 50 % (LDF) exceeded 0.4 mg/L manganese (max. 6.6 mg/L). None of the water samples located outside the actual floodplain of sediment-rich rivers, or on riverbanks of sediment-poor rivers exceed 5 μg/L As, and only 4 % exceeded 0.4 mg/L Mn. The areas of highest risk can be delineated using satellite imagery. We observe similar patterns as in affected river basins in South and Southeast Asia indicating a key role of sedimentation processes and fluvial geomorphology in priming arsenic and manganese contamination in aquifers.

* Corresponding authors.
E-mail addresses: demeyerc.caroline@gmail.com (C.M.C. de Meyer), iwahnfried@ufam.edu.br (I. Wahnfried), jrodriguez@uni.edu.pe (J.M. Rodriguez Rodriguez), rolf.kipfer@eawag.ch (R. Kipfer), pagarcia@uni.edu.pe (P.A. García Avelino), ecarpiod@uni.edu.pe (E.A. Carpio Deza), michael.berg@eawag.ch (M. Berg).
[1] Present address: Soil Science Unit, Institute of Geography, University of Bern, 3012 Bern, Switzerland.

http://dx.doi.org/10.1016/j.scitotenv.2022.160407
Received 19 August 2022; Received in revised form 15 November 2022; Accepted 18 November 2022
Available online 24 November 2022
0048-9697/© 2022 The Authors. Published by Elsevier B.V. This is an open access article under the CC BY license (http://creativecommons.org/licenses/by/4.0/).

1. Introduction

Deltas and alluvial plains of large rivers sourced in Cenozoic mountain belts are typical areas of concern for groundwater arsenic contamination worldwide (Ravenscroft et al., 2009; Podgorski and Berg, 2020). Within the river basins a marked heterogeneity in arsenic groundwater concentrations has been observed at different scales (Smedley and Kinniburgh, 2002; van Geen et al., 2006; Weinman et al., 2008; McArthur et al., 2011). On a regional scale, bed-rock geology and related relief delineates the affected zone, which is typically limited to flat areas containing poorly drained late-Quaternary alluvial sediments (Buschmann et al., 2007; Winkel et al., 2008). On a more local scale, within late-Quaternary deltas and alluvial plains, the heterogeneity in arsenic-concentration has been related to the fluvial morphology (Acharyya et al., 2000; Acharyya and Shah, 2007; Papacostas et al., 2008; Weinman et al., 2008; Nath et al., 2008; Stahl et al., 2016; Das and Mondal, 2021; Kazmierczak et al., 2022). It has been suggested that fluvial dynamics causes irregular patterns in the local stratigraphy on a meter to kilometer scale, which affects the groundwater arsenic-distribution. Fluvial dynamics has a direct control on sediment burial age (Postma et al., 2012), sediment deposition rate, flow rate, and indirectly on the availability of reactive organic matter and iron (hydr)oxides (McArthur et al., 2004; Meharg et al., 2006; Kocar et al., 2008; Papacostas et al., 2008; Quicksall et al., 2008; Stuckey et al., 2016; Magnone et al., 2017; Donselaar et al., 2017; Jakobsen et al., 2018), factors that control arsenic mobility in aquifers. Within a single aquifer, local flow patterns, and heterogeneous aquifer sediments can cause vertical and horizontal concentration gradients (McArthur et al., 2004; van Geen et al., 2013; Radloff et al., 2017). This natural variability can be biased by anthropogenic influence, whether by direct intervention in the landscape (e.g. as in Weinman et al., 2008), or by induced groundwater flows, through increased pumping, enhancing arsenic mobilization in formerly uncontaminated aquifers (Harvey et al., 2002; Winkel et al., 2011; Erban et al., 2013; Zhang et al., 2020). Understanding the natural heterogeneity is key to mitigation strategies of affected regions for drinking water supply.

Arsenic concentrations up to 700 μg/L - far above the current WHO guideline value of 10 μg/L (WHO, 2011) - have recently been recorded in groundwater resources of the Peruvian Amazon (Rebata-H et al., 2009; de Meyer et al., 2017). For the Amazonian population (~28 Million people, FAO (2015)), groundwater is an important resource, despite the presence of abundant surface water. Globally, the negative health impact of chronic arsenic intake through contaminated water consumption has been well documented (Smith et al., 2000; Kapaj et al., 2006; Bundschuh et al., 2022). The detection of such high values in the Amazon region calls for basin-wide and in-depth investigation on the presence and distribution of arsenic in groundwater resources.

In a pilot study on the hydrochemical characteristics of the groundwater in the Peruvian Western Amazon, de Meyer et al. (2017) proposed that the arsenic is of geogenic origin and that its mobilization is compatible with microbially induced reductive dissolution of iron and manganese (hydr-)oxides. The contaminated groundwater resources are located in recent alluvial deposits along the Amazon River and its main headwaters. They showed that the elevated arsenic concentrations occur in shallow aquifers in young floodplains of sediment-laden rivers of Andean origin. In these areas of rapid sedimentation, the key environmental conditions for mobilization of arsenic under reducing subsurface conditions are met, consisting of late-Quaternary sediments with high loads of organic matter (McArthur et al., 2004; Meharg et al., 2006; Postma et al., 2012).

In recent years, manganese attracted considerable attention in groundwater studies, especially the simultaneous occurrence of arsenic and manganese at concentrations potentially harmful to human health in groundwater of a single affected area (Wasserman et al., 2006; Buschmann et al., 2007; McArthur et al., 2012; Ying et al., 2017). In the floodplains of the Peruvian Western Amazon manganese exceeded the current WHO health-based value of 0,4 mg/L (WHO, 2011) in 80 % of the shallow wells, and in 100 % of the wells with arsenic above 10 μg/L (de Meyer et al., 2017). Maximum concentrations attained 10 times the WHO-guideline value, a limit that is already considered as too high by e.g. Wasserman et al. (2006), Frisbie et al. (2012), Kullar et al. (2019) and Mitchell et al. (2021).

Here we present a first comprehensive hydrochemical survey of shallow groundwater resources in the floodplains of the lowland Western and Central Amazon Basin. The spatial distribution of arsenic and manganese contamination within the watershed is investigated by testing the effects and scales of fluvial heterogeneity and dynamics on geogenic groundwater contamination throughout the Amazon Basin. We focus on the spatial variability in riverine areas, with particular emphasis on the distribution on the floodplain scale. Finally, we discuss the fluvial dynamics as a controlling mechanism for the distribution of arsenic and manganese.

2. Geomorphological characteristics of the Amazon basin

The Amazon Basin is the biggest watershed on earth. It is a vast and heterogeneous region with a widely varied geological and geomorphological history. It extends from the relatively young tectonically active mountain chain of the Andes in the west to a geologically very old substrate of Precambrian shields in the east, covering an area of about six million km^2, corresponding to about one third of the South-American continent (Fig. 1). The uplift of the Andes has resulted in a dynamic fluvial system, with large areas of the western and central Amazon being covered by Cenozoic sediments (Hoorn et al., 2010; Mora et al., 2010). The headwaters of the Amazon River drain a major part of the Northern and Central Andes, which are to date prone to strong erosion (Aalto et al., 2006; Latrubesse and Restrepo, 2014). As a result, the Amazon River carries the highest sediment load on earth, with total suspended solids of almost 0.9 Gt/a discharged into the Atlantic Ocean (Filizola et al., 2011 and references therein). More than half of the Andean sediment discharge is trapped in the foreland basins and along the floodplains (e.g. Meade et al., 1985; Guyot, 1993; Dunne et al., 1998; Mertes et al., 1996; Aalto et al., 2006; Filizola and Guyot, 2009). The foreland basins, located just east of the Andes (Fig. 1), are structurally-driven subsiding sedimentary basins filled with up to 5000 m thick piles of Late Cretaceous and Cenozoic sediments (Dumont and Fournier, 1994; Dumont, 1996; Mora et al., 2010). Tectonic and sedimentary studies indicate that the Amazon region was a dynamic depositional environment throughout the Quaternary, with frequent shifting of river courses (Räsänen et al., 1987; Dumont, 1991; Rossetti et al., 2014; Rossetti, 2014; Lombardo, 2014; Ruokolainen et al., 2019; Pupim et al., 2019).

From the base of the Andes towards the east, the entire Amazon basin has a relatively flat relief (e.g. Mertes and Dunne, 2007). For example, the city of Iquitos lies 3600 km from the ocean, with the elevation of the Amazon River being only 85 m.a.s.l.. The elevation of the Amazon River at Manaus, 1500 km from the ocean, is just 15 m.a.s.l. during the low season. The northern and northwestern parts of the Amazon Basin have a tropical climate with a yearly rainfall of 2000 to 6000 mm/year (this is the case for study region A), whereas the east and particularly the south experience distinct dry (Apr.–Oct.) and wet seasons (Nov.–Apr.) (study regions B and C) (Espinoza Villar et al., 2009). Originating from the time-dependent rainy seasons in the northern versus central Andes, two annual flooding events occur in the westernmost Amazon Basin. In our studied regions, the rising of the Amazon and its head-waters starts around September–October, being delayed downstream to reach its peak between May and July before the confluence with the Negro river, west of Manaus (Filizola et al., 2011). The Marañon river's peak discharge is attained about two months earlier. The rise and fall of the rivers result in a fluctuation of local and regional water base levels, which directly influence the groundwater table and soil formation.

Reflecting the environment in which the rivers originate, different river types drain the Amazon Basin, varying in their sediments loads and -types,

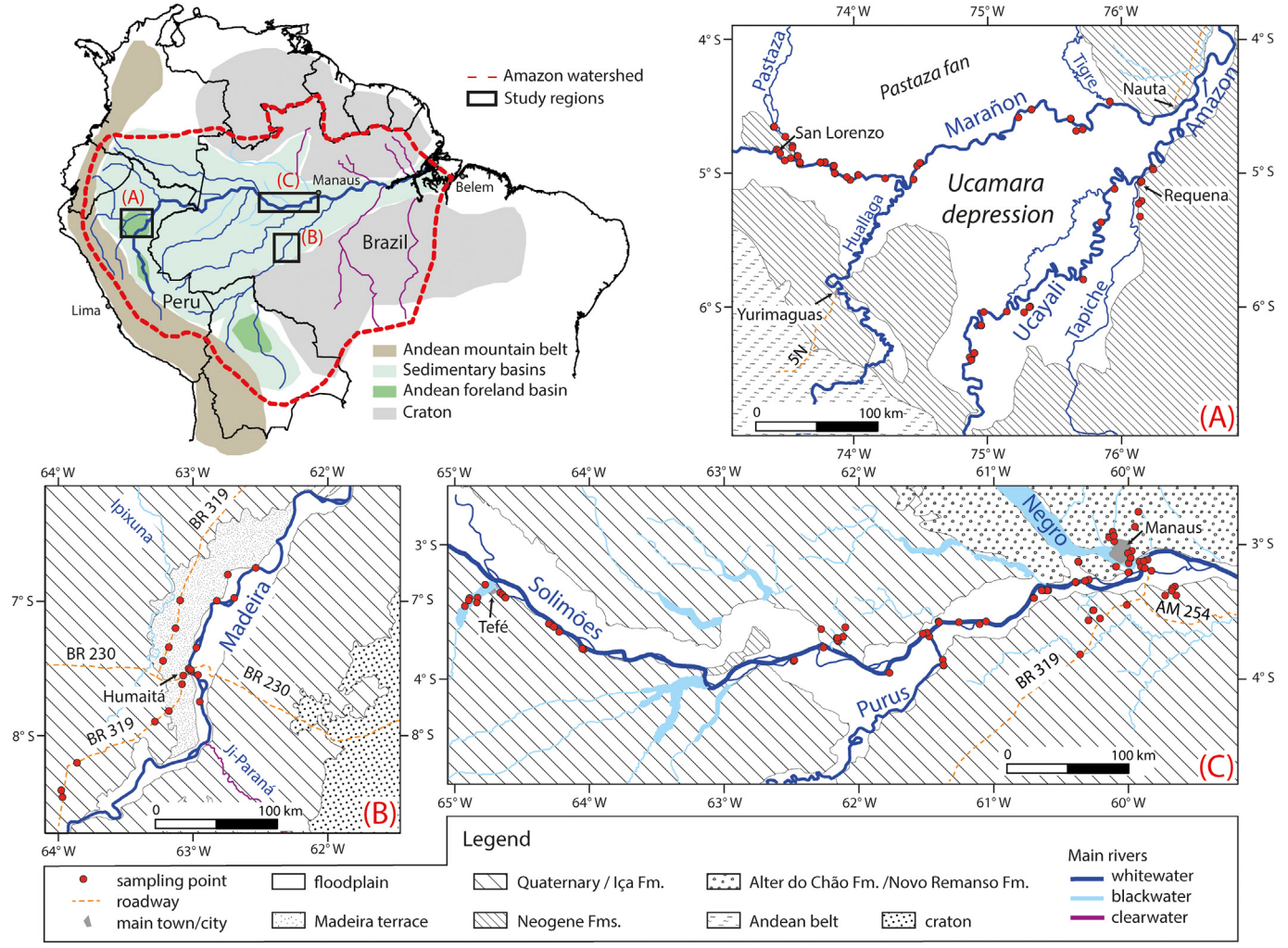

Fig. 1. Overview of the studied regions and sampling points in the Amazon Basin, South-America. Upper left: tectonic sketch of the Amazon watershed with indication of the study regions. Geological sketches of the study regions with indication of the sampling points: (A) Ucamara depression in Peru; (B) central Madeira River in Brazil; (C) Solimões River in Brazil (this stretch of the Amazon River from the Brazilian border up to its confluence with the Negro River is locally called Solimões River).

as well as in dissolved organics (Sioli, 1956; Gibbs, 1967; McClain and Elsenbeer, 2001; Junk et al., 2011). The sediment-laden rivers originating in the Andean highlands are called whitewater or Andean rivers. In the lowlands, these whitewater streams merge with sediment-poor blackwater rivers (e.g., the Negro River which flows into the Amazon River at the city of Manaus, Fig. 1C). They contain less sediments, but high loads of organic matter. Further east, clearwater rivers drain the Brazilian and Guiana shields (Fig. 1). The geological substrate and this dynamic river system divide the Amazon Basin into the floodplains, which border the main channels and are subject to annual flooding, and the elevated terraces that lie above the levels of inundation. The floodplains are known as várzea (Portuguese) or llanura (Spanish) for Andean floodplains, versus igapó for blackwater environments. Whereas the elevated terraces are locally called Terra Firme. The annually flooded soils of Andean rivers are poorly drained and are fertile because of the resulting annual deposition of fresh silt (e.g. Puhakka et al., 1992).

3. Methods

The study comprises large regions in both the Western and Central Amazon, focusing on groundwater resources of riverine settlements along various Amazonian tributaries, in Peru and Brazil. Groundwater and river water were collected and analyzed for a broad range of hydrochemical parameters. The sampling points for groundwater were then located for their position within the river basin, using field observations, regional geology, maps and remote sensing data, mainly digital elevation model (DEM) from the Shuttle Radar Topography Mission (SRTM), to decipher systematic correlations between groundwater chemistry and fluvial geomorphology.

3.1. Sampling

Groundwater samples were collected during three field campaigns from tube wells in riverine settlements and households (151 locations). Surface water from lakes and rivers (20 locations) were collected for comparison. The three studied areas range over several hundreds of square kilometers and comprise both seasonally flooded riverbanks and non-floodable terraces in Western and Central Amazonia in Brazil and Peru, along the Amazon River and some of its major tributaries (i.e. the Ucayali, Marañon and Madeira rivers, Table S.I.1 and Fig. 1).

Samples from tube wells were taken in every place where a pump in working condition was available. The investigated wells ranged from 12 to 110 m depths. Sampling in the Ucamara depression in Western Amazonia in Peru (study region A), along the Ucayali River and the Marañon River (Fig. 1A) was done during a two weeks river-cruise in early September 2017, corresponding to the end of the low water river stage. Sampling along the Madeira River in Brazil (study region B) in the area of Humaitá (Fig. 1B) was done both by car and boat transport in May 2016,

corresponding to the end of the rising stage. Sampling along the main Amazon River in Central Amazonas in Brazil (Fig. 1C) (locally called Solimões River, study region C) was first accomplished during a one week field campaign by boat and car transport from the city of Manaus during May 2016, and a three weeks boat cruise during October–November 2017, corresponding to the end of the rising stage and to the start of the rising river water, respectively.

3.1.1. Tube wells

Each well was flushed by manual or electrical pump for at least 10 min, until attainment of stability of physicochemical parameters (pH, T, O_2, EC and Eh), which were measured using a portable multi-analyzer (WTW Multi 340). Eh values reported in this study have been normalized to the standard hydrogen electrode. The duration of pre-pumping was recorded, and it is indicated in the results table (Table S.I.2) if drying-out of the well was prominent, and hence sampling was done before complete flushing. Organoleptic observations were also registered. Information on the construction of the well, if available, were obtained from well owners or local authorities. Three aliquots of fresh water were collected in polypropylene (PP) flasks per well: (1) 250 mL for analysis of major ions, alkalinity, total hardness, total inorganic nitrogen, ortho-phosphate, dissolved organic carbon (DOC), and total organic carbon (TOC) was collected unfiltered and non-acidified; (2) 30 mL for analysis of trace elements, total and ortho-phosphate and ammonium, that was filtered in-situ through a disposable 0.45 μm cellulose acetate filter and acidified with supra pure 10 M HNO_3 to attain a 1–2 pH; (3) 30 mL as in (2), but additionally filtered with a disposable cartridge for arsenic speciation (Meng and Wang, 2008).

3.1.2. Rivers and lakes

Water samples from lakes and rivers were collected manually from a small outboard engine boat, in locations in the middle of the stream or at least 40 m away from the margins, with a bucket or bottle about one arm length (~1 m) below the water surface. Aliquots were taken as for tube well water.

All samples were transported by airplane to the Swiss Federal Institute of Aquatic Science and Technology (Eawag) in Switzerland for analysis. Whenever possible, the samples were kept cooled and stored at 4 °C in the dark prior to analysis. This means that the samples were without cooling for a maximum six days and were stored in the dark immediately after sampling.

3.2. Chemical analysis

The concentrations of major cations and trace elements were measured by inductively coupled plasma mass spectrometry (ICP-MS); ammonium, ortho-phosphate, and silicic acid by photometry; major cations, and anions by ion chromatography; total inorganic nitrogen with chemo luminescence; DOC (after pre-filtration with 0.45 μm cellulose acetate filter) and TOC with a carbon-analyzer by catalytic combustion at 720 °C; and alkalinity and total hardness by titration in the laboratory. For samples with measured total arsenic concentrations above 1 μg/L, the aliquot filtered for arsenic speciation was analyzed by ICP-MS for determination of the arsenite concentration. Analytical procedures and robustness tests are as described in de Meyer et al. (2017). Cross-evaluation between ICP-MS and ion chromatography analysis of the main cations, within two different aliquots for each sample, resulted in correlation coefficients (r^2) ≥0.98, except for calcium, that was partially precipitated in the non-filtered, non-acidified samples of very reduced well-water. The limits of quantification (LOQ, 10 × standard deviation of noise) are listed in the Supplementary Table S.I.2 and were 0.5 μg/L, respectively 0.01 mg/L, for arsenic and manganese. For more information on quality assurance and data validation we refer to Berg et al. (2008) and Winkel et al. (2011).

3.3. Location of sampled wells within the river basin's structural units

To date, the geochronology and stratigraphy of the youngest sedimentary episodes in Amazonia is poorly constrained. Therefore, we complement available geological data (for references see chapter 4) with geomorphological features visible on spatial data, using the Digital Elevation Model (DEM) derived from the Shuttle Radar Topography Mission (SRTM) (DEM SRTM v.2) and satellite imagery, to determine the location of the wells within the structural parts of the river subbasins. In a first step we differentiate between wells from riverine settlements lying inside the different parts of the actual floodplain and those on higher-lying, older terraces (Terra Firme). In a second step, within the floodplains of whitewater rivers, we differentiate between erosional and depositional parts of the floodplain with different water and sediment dynamics. In detail we distinguish between areas inside and outside the influence of the actual whitewater river channels (in analogy to Mertes et al., 1996; Latrubesse and Franzinelli, 2002). The channel-dominated area (CDF) is the dynamic part of the floodplain where scrolls, levees, (filled) oxbow lakes, and (abandoned) channels remain visible on the DEM-image demonstrating recent channel-migration. This is different in the less-dynamic component of the floodplain (LDF) that is not influenced by the actual channeling, but undergoing regular flooding. This part of the floodplain is characterized by flat surfaces and lakes, and is only partially affected by seasonal flooding, resulting in low sedimentation.

4. Study regions

4.1. Selection of the study regions

In the Peruvian Amazon, arsenic enrichment in groundwater was documented in the floodplains of whitewater rivers, but not in the blackwater environments (de Meyer et al., 2017). This study is therefore focused on the riverbanks of whitewater environments. We investigated three different parts of the Amazon Basin (Fig. 1) to test for possible contrasting behavior of different sedimentary environments. With increasing distance from the Andean mountain chain the investigated regions are (Fig. 1): (A) Study region A (Ucamara depression) in Western Amazonas as an example for a foreland basin, a highly dynamic sedimentary environment, first zone of high sediment deposition, just east of the Andes; (B) Study region B (central Madeira River) in Central Amazonas, along the Madeira River, the Amazonian tributary with the highest suspended sediment-load. After confluence of its head-rivers by leaving the subandean Bolivian foreland basin, and flowing on the Brazilian shield, shifting of the Madeira river resulted in an area of recent deposition, forming several terraces. (C) Study region C (Solimões River) in Central Amazonas, along the 600 km long stretch between Tefé and Manaus. In this area several blackwater streams join the Amazon river in which different stages of floodplain formation can be investigated.

4.2. Study region A: Ucamara depression

The Marañon and the Ucayali River flow through the Ucamara depression, before their confluence to form the main Amazon River (Fig. 1A). The Ucamara depression, corresponding to the central part of the (Pastaza-) Marañon Basin (Dumont and Garcia, 1991; Dumont and Fournier, 1994), is an actively subsiding foreland basin, in which high sedimentation from Andean provenance is taking place (Räsänen et al., 1987, 1990, 1992; Dumont and Fournier, 1994; Dumont, 1996; Roddaz et al., 2005). The alluvial sediments are deposited by rapid river channel migration, resulting in an alternation of massive layers of clays, silty clays, fine sands and peat. The whole flat area is commonly referred to as a mosaic of Holocene and late-Pleistocene alluvial, fluvial and palustrine deposits (INGEMMET, 1999; Martínez et al., 1999; De La Cruz et al., 1999; Guzmán et al., 1999; INGEMMET, 2016). Data on age and thickness of the sediments are scarce. Radio-carbon dating of riverbanks of the meander belt of the Ucayali River resulted in late-Holocene ages from 140 to 2720 yBP (Dumont and

Fournier, 1994). Two ^{14}C ages on a terrace at the border of the Ucamara depression gave late-Pleistocene ages of 40,000 and 13,000 yBP indicating that all visible fluvial signs are younger than 13,000 years (Dumont et al., 1988). Abundant peatland, which are Holocene in age at least to a depth of 7.5 m, is partially covered by overbank deposits (Lähteenoja and Page, 2011; Lähteenoja et al., 2012).

The Marañon River is bordered to its north by Pastaza fan sediments (Fig. 1A). Mainly blackish andesitic volcanoclastic debris are deposited by its northern tributaries, such as the Pastaza River, originating in the volcanic area of the Ecuadorian Andes (Räsänen et al., 1992; Bernal et al., 2011, and references therein). The sediments are considered to be late-Pleistocene to Holocene in age, consisting of coarse to fine grained dark grey sands, with lighter colored layers at the base, and containing some organic carbon-rich layers with trunks and remnants of plants. The lithic fragments are low to moderately oxidized. In vast areas these deposits are covered by an organic-rich soil. This whole area is low-lying and gets seasonally flooded by the rivers and rain (INGEMMET, 1999; Martínez et al., 1999; Quispesivana et al., 1999).

To the east and south, the Ucamara depression is bordered by Neogene sedimentary rocks, forming a hilly relief. Further west, the steep, eastern slope of the Andean belt results in exposed Cretaceous rocks (see Fig. 1A).

4.3. Study region B: central Madeira River

The Madeira River is the largest tributary of the Amazon River (Dunne et al., 1998) when considering both sediment-load (430–450 Mt/y; Vauchel et al., 2017) and discharge (average discharge of about 31,200 m^3/s; Leite et al., 2011). The headwaters of this river originate in the Central Andes and on the Brazilian shield. Part of their high sediment load gets deposited and reworked in the Bolivian foreland basin (Aalto et al., 2006). After confluence of its headwaters, the channel of the Madeira River narrows and flows over the Brazilian shield (Fig. 1). In its middle-course (around the city of Humaitá) the alluvial plain of the Madeira River gets considerably wider (Fig. 1B) and flows through large Quaternary fluvial terraces originating from neotectonic activity (Bahia and Oliveira, 2004; Rossetti et al., 2014; Hayakawa and Rossetti, 2015). In the actual floodplain (T3 in Rossetti et al., 2014), the fluvial deposits of late-Pleistocene to Holocene age display paleo-meander loops and scroll-bar morphology (Rossetti et al., 2014; Bertani et al., 2015; Hayakawa and Rossetti, 2015). To the northwest, the actual floodplain is bordered by a former fluvial terrace (T2 in Rossetti et al., 2014), referred to as Madeira terrace in Fig. 1. Paleo-lakes formed by blocking of the channel (paleorias) on this late-Pleistocene terrace are filled with up to 9 m thick fine-grained sediments, mainly red clay with dispersed plant remnants of late-Pleistocene to Holocene age (Rossetti et al., 2014; Bertani et al., 2015). The higher lying hilly relief corresponds to older terraces of the Içá formation, which is composed of iron-rich sandstones, siltstones and clays, and some lenses of peat (Bahia and Oliveira, 2004; T1 in Rossetti et al., 2014).

4.4. Study region C: Solimões River

The Central Amazon is a large depression in which the Amazon River -named Solimões River in Brazil, up to its confluence with the Negro River - flows between Cenozoic terraces, before narrowing its channel at the confluence with the Negro River. Hereafter, the Amazon River is bordered by more elevated Mesozoic (Cretaceous) terraces (Faria et al., 2004), where the sedimentary basin is straddled by the Brazilian and the Guiana shields (Fig. 1). The course of the Amazon River is influenced by neotectonics and reactivation of ancient structural arches (Mertes et al., 1995; Latrubesse and Franzinelli, 2002; Latrubesse et al., 2010). The Pleistocene sea-level and precipitation changes controlled fluvial dynamics, resulting in a deep channeling of the Negro and Amazon River. The subsequent dominant infilling of the Amazon channel with respect to the Negro river channel is caused by significant differences in sediment supply (Silva et al., 2007). At least up to Manaus, deep incision of the rivers during the Last Glacial Maximum is recorded. Within our study region, i.e. the 600 km long stretch between Tefé and Manaus (Fig. 1C), the modern floodplain of the Amazon River is bordered by ria lakes. These lakes are the outflows of blackwater rivers that are blocked by the Amazon River. Along this section, several generations of fluvial terraces have been identified (Mertes et al., 1996; Latrubesse and Franzinelli, 2002; Gonçalves Júnior et al., 2016; Bezerra et al., 2022). In the last decade, regional studies have aimed to determine the geochronology of the evolution of these terraces. Up to date, age determinations are mainly limited to exposed riverbanks. OSL age determinations of the terraces outside of the actual floodplain systematically resulted in late-Pleistocene ages between 20,000 to 200,000 y (Gonçalves Júnior et al., 2016; Pupim et al., 2019; Passos et al., 2020; and references therein). OSL age determinations of exposed riverbanks within the floodplain of the Solimões River and on its islands resulted in mainly Holocene to exceptionally late-Pleistocene ages (from 750 to 18,000 yBP), as well as Holocene radiocarbon ages of exposed plant debris (300–2500 yBP) (Latrubesse and Franzinelli, 2002; Soares et al., 2010; Rozo et al., 2012; Gonçalves Júnior et al., 2016; Pupim et al., 2019; Passos et al., 2020).

5. Results

Concentrations of arsenic ranged from <0.5 μg/L (below the limit of quantification LOQ) to 430 μg/L. With a few exceptions, total arsenic corresponded to As^{III}-concentrations (see Table S.I.2). Manganese-concentrations ranged from <0.01 mg/L (<LOQ) to 6.6 mg/L. In acidic groundwater with a pH ≤ 4.2, aluminum-concentrations of up to 2.6 mg/L were detected in wells located in blackwater environments, as observed in earlier studies (de Meyer et al., 2017). Frequently, iron and phosphate, and in isolated cases, concentrations of barium, zinc, led and nitrate exceed the current WHO-guideline values (WHO, 2011; in bold in Table S.I.2).

5.1. Spread of arsenic and manganese in groundwater

5.1.1. Study region A: Ucamara depression (Western Amazonia, Peru)

Groundwater from 56 tube wells from riverine settlements along the headwaters of the Amazon River, i.e. the Marañon and Ucayali Rivers were collected. Additionally, wells along the smaller Pastaza River, a whitewater tributary of the Marañon River, and along the Tapiche River, a smaller tributary of the Ucayali River, were also sampled (see Figs. 1A & 2a). The depth of the wells varies between 12 and 70 m. Arsenic-concentrations vary between <1 and 240 μg/L, whereby one out of three show arsenic-concentrations above the WHO-guideline of 10 μg/L (WHO, 2011). Manganese-concentrations vary from the limit of quantification (<0.01 mg/L) to 6.6 mg/L, with about 40 % of them exceeding the current WHO health-based value of 0.4 mg/L (WHO, 2011).

In the study region A shown in Fig. 2a, the floodplain and the higher topographic areas are distinguished by elevation (DEM-SRTM). Within the alluvial plain of the Ucamara depression, we also separated between the channel-dominated parts of the main rivers and the rest of the floodplain. All tube wells located on older deposits, corresponding to higher topographic areas, (Terra Firme) -that is mainly along the Tapiche River and around San Lorenzo- as well as the tube wells along the Pastaza River tap groundwater with low arsenic-concentrations (<5 μg/L). All wells with arsenic-concentrations above 10 μg/L are located on the floodplains of the Ucayali and Marañon Rivers. Most wells with arsenic concentrations exceeding 10 μg/L and manganese concentrations exceeding 1 mg/L are located on the channel-dominated parts of the floodplains (CDF) (orange stripes in Fig. 2). There is a clear difference in arsenic-concentrations between the wells on the CDF of the Ucayali versus the Marañon River. High arsenic-concentrations (>50 μg/L) are located on the Ucayali CDF, whereas a somewhat lower range (10–50 μg/L) is found in groundwater on the CDF of the Marañon River (Figs. 2a, 3a and Table 1).

Shallow well water in the less-dynamic part of the floodplain (LDF) of the Marañon River is also enriched in arsenic and manganese, as shown in the data plotted in Fig. 3a. This is illustrated in a schematic cross section

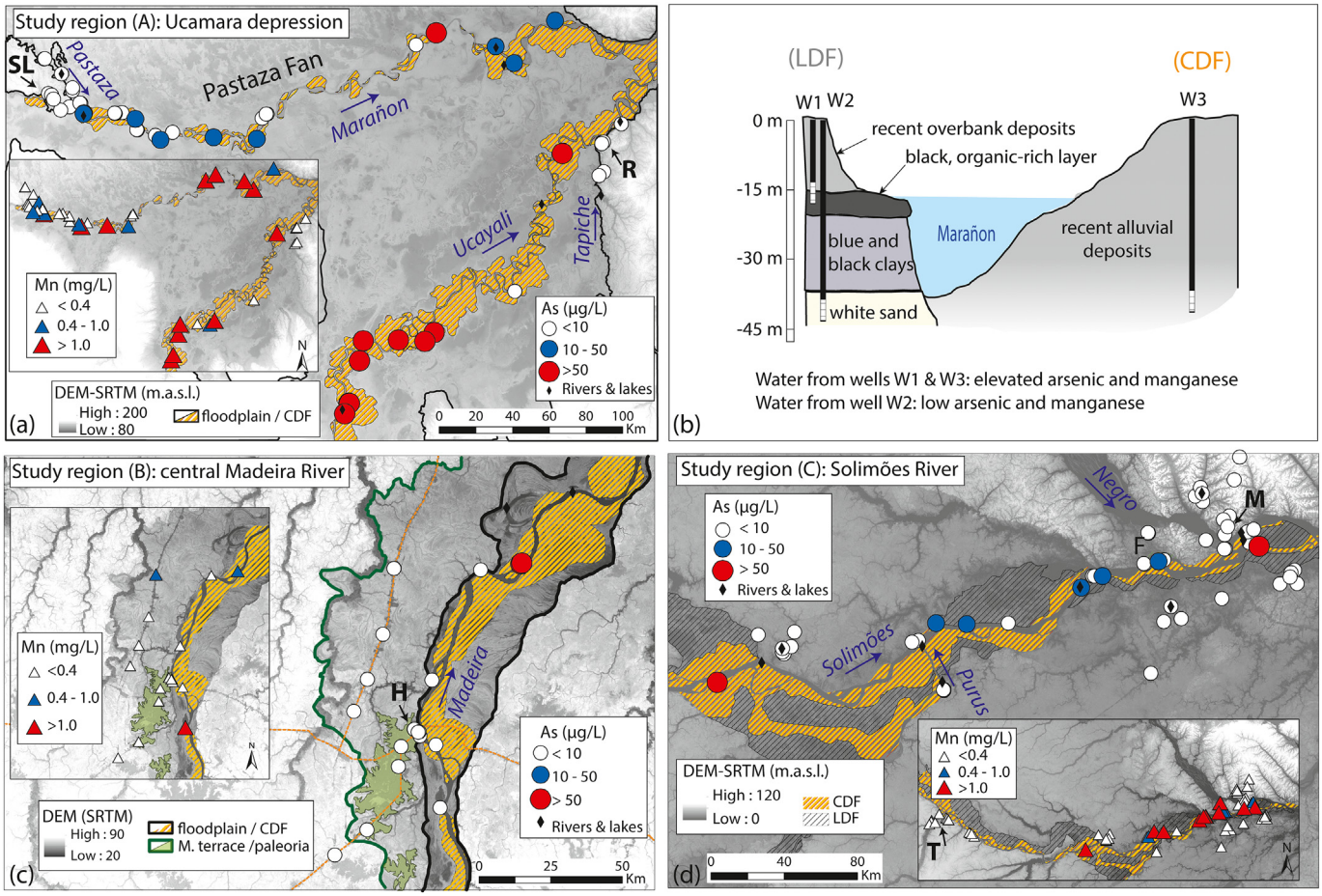

Fig. 2. Span of arsenic and manganese concentrations of wells in the studied regions. The background of the maps in a, c & d corresponds to the DEM-SRTM. (a) The channel-dominated part of the floodplains (CDF) of the Ucayali and Marañon rivers is highlighted. The CDF of the Ucayali River is significantly larger than of the Marañon River. Used symbols: SL = San Lorenzo; R = Requena. (b) Schematic cross-section of the floodplain of the Marañon River, indicating spatial variability in groundwater quality on opposite riverbanks. The sketch is based on field-observations and information from well owners. In some places, the black organic-rich layer was outcropping at the moment of our sampling campaign, and trunk and leaf rests were clearly visible. Information on the kind of sediments in deeper parts of the CDF is missing. Wells of all depths on the CDF -hence on the riverbank with sediment deposition- tap arsenic-enriched groundwater. On the erosive riverbank, only the shallow wells reaching the overbank deposits or underlying organic-rich layer tap arsenic-enriched groundwater. (c) The youngest CDF of the Madeira River is highlighted on the map. The paleorias are visible as flat dendritic textures. Three tube-wells that we sampled (tapping water with concentrations of As < 10 µg/L and Mn < 0.4 mg/L) along the road to Porto Velho, are located outside of the southwestern part of the map illustrated here (see Fig. 1B). Used symbols: H = Humaitá. (d) The CDF and the less-dynamic part of the floodplain (LDF) of the Solimões and the Purus River are highlighted. For graphical purposes, 13 of the sampled tube wells, all tapping groundwater with concentrations of As ≤ 1 µg/L and Mn ≤ 0.2 mg/L, on the higher southern terrace of the Solimões River and along Lake Tefé, are only illustrated on the Mn-inlet. Used symbols: T = Tefé; M = Manaus; F = paleo-channel of the Negro River.

through the riverbanks at opposite sides of the Marañon River (Fig. 2b). During the sampling campaign we observed that on the erosive bank of the river, a layer of overbank deposits covers a few meters thick blackish, organic-rich coarse layer, containing buried plant remains, above a greyish-whitish clay layer. Shallow wells reaching the overbank deposits or this organic rich layer (W2 on Fig. 2b), tap groundwater with elevated arsenic and manganese concentrations. Deeper wells (W1 on Fig. 2b) tap water of deeper aquifers that are generally low in these contaminants (As <1–10 µg/L; and Mn < 0.4 mg/L; see Fig. 3a). This is in contrast to wells of the same depth, but located on the opposite bank of the river, where active sedimentation takes place (W3 on Fig. 2b) and where concentrations are high.

5.1.2. Study region B: central Madeira River (Central Amazonia, Brazil)

Water from 23 tube wells of 12 to 80 m depth were sampled in settlements along the Madeira River, in the city of Humaitá, and along highway BR-319, respectively 60 and 140 km to the north and south of the city (Fig. 1B). Higher topographic areas and the floodplain of the Madeira River are distinguished in Fig. 2c. Within the modern floodplain of the Madeira River, several generations of meander belts can be recognized. Only the youngest generation of the floodplain, currently under the influence of the active channel is considered as CDF (orange stripes in Fig. 2). On the Madeira terrace the paleorias are visible as flat dendritic textures. From the 23 well-waters sampled in this study area, most have very low arsenic-concentrations (<1 µg/L), including all the wells on the Madeira terrace (Figs. 3b & 2c). Only a few wells on the floodplain could be sampled, because many have been destroyed by the extreme flood of 2015. Water from two wells, about 30 m deep, located on the CDF were contaminated with 300–400 µg/L arsenic.

The majority of manganese-concentrations vary from <0.01 to 0.4 mg/L. One well located on the modern floodplain but outside of the CDF taps water with manganese-concentrations of 3.4 mg/L. The wells reaching deeper than 33 m and located on the CDF tap groundwater from a deeper aquifer, below a red, hard layer (see indication in Table S.I.2). Here, arsenic and manganese are not accumulated in the groundwater (see Fig. 3b).

5.1.3. Study region C: Solimões River (Central Amazonia, Brazil)

In our studied region along the main stem of the Amazonas River several features of the floodplain are visible on the SRTM-DEM image (Fig. 2d),

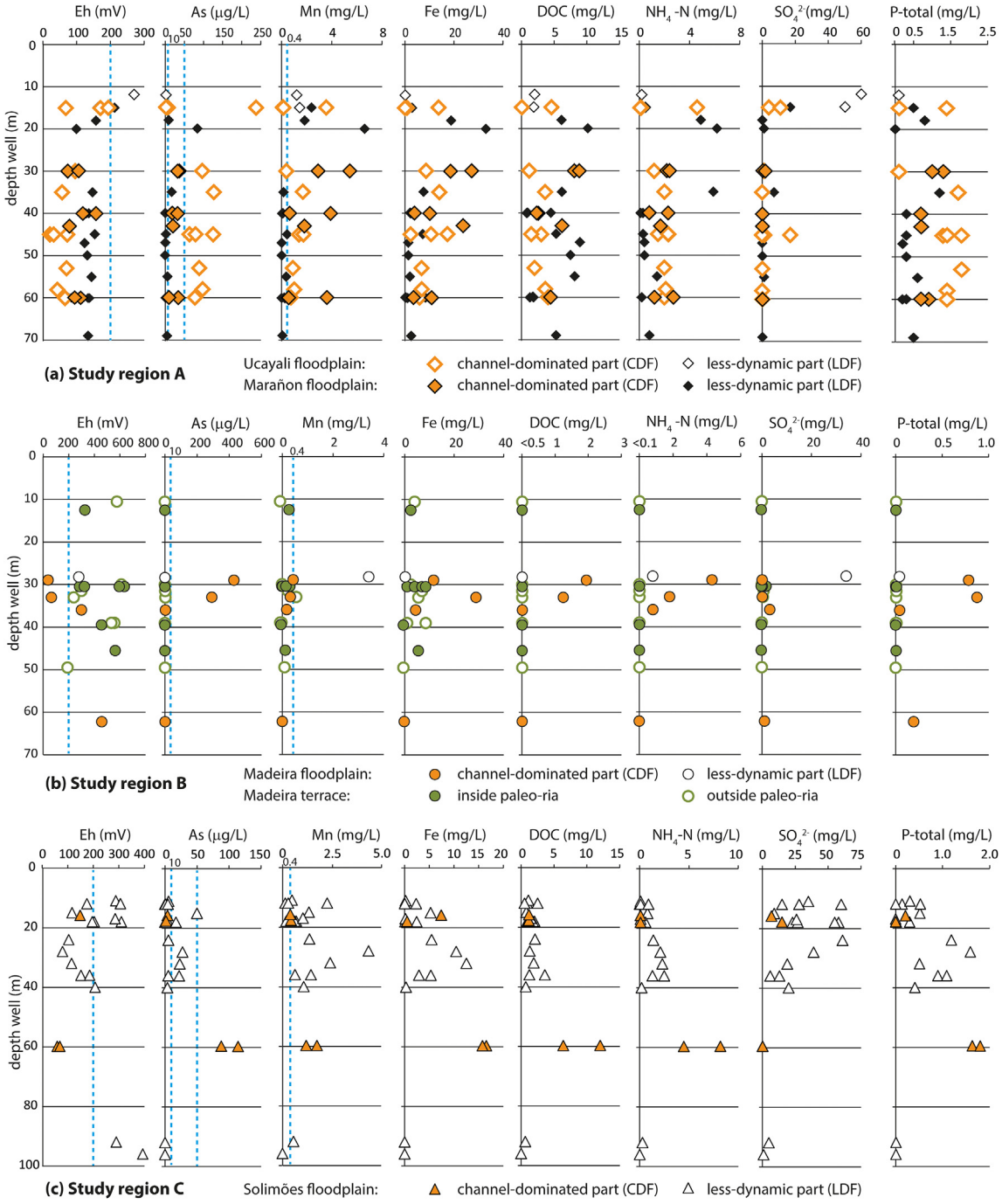

Fig. 3. Hydrochemistry of groundwater versus depth of the wells sampled on the floodplains within the studied regions. (a) floodplains of the Marañon (filled symbols) and Ucayali River (open symbols). (b) floodplain (orange symbols for CDF, white symbols for older part) and terrace (green, round symbols) of the Madeira River; (c) floodplain of the Solimões River (filled symbols for CDF and open symbols for LDF).

where the two different geomorphological units within the modern floodplain are indicated. Beside the channel-dominated floodplain (CDF), which is the dynamic part of the floodplain, we distinguish the less-dynamic part of the floodplain (LDF), in analogy with the impeded floodplain of Latrubesse and Franzinelli (2002). The boundary of the LDF with the CDF or river features a levee that blocks the flow of the lakes towards the main channel. We defined the limits of the modern floodplain with the higher terraces, where the modern fluvial ria lakes enter on the plain.

Water from 72 tube wells from riverine settlements and households along the Amazon River, various lakes and side-channels, the Purus River as well as in the city of Manaus were sampled (Fig. 1C). All wells located outside the floodplain of the Amazon River are tapping groundwater with arsenic-concentrations <5 µg/L and manganese ≤0.4 mg/L. Exceptions are wells on the (former) floodplain of the Negro River, where higher manganese concentrations up to 2 mg/L were detected. Only few wells were sampled on the CDF. All tube wells tapping groundwater with arsenic concentrations above 10 µg/L, up to 115 µg/L, are located on the floodplain of the Amazon River, both on the CDF and the LDF. A difference in depth of the wells versus arsenic concentration is recognized (Fig. 3c). The deeper wells on CDF tap groundwater with arsenic above 50 µg/L, and manganese above 1 mg/L, whereas the wells between 18 and 35 m depth on the LDF tap groundwater with arsenic-concentrations below 50 µg/L, and manganese-concentrations above 1 mg/L (Fig. 3c). According to the descriptions from the well-owners, the very shallow wells on the CDF are

Table 1
Overview of arsenic and manganese concentrations of groundwater for the different structural parts of each studied river basin (CDF = channel-dominated part of the floodplain; LDF = less dynamic part of the floodplain).

	Number of wells	Depth well (m)	As (μg/L)			Mn (mg/L)		
		Range	Range	Median	>10 μg/L (%)	Range	Median	>0.4 mg/L (%)
Region A	56	12–73	<1–240	2	32	0.01–6.6	0.3	41
CDF	18	15–60	2–240	50	89	0.1–5.4	1.4	83
Ucayali River	*11*	*15–60*	*2–240*	*90*	*82*	*0.1–3.6*	*1.0*	*73*
Marañon River	*7*	*30–60*	*10–36*	*31*	*100*	*0.6–5.4*	*2.9*	*100*
LDF	25	12–69	<1–84	1	12	0.01–6.6	0.2	32
Ucayali River	*2*	*12–15*	*1–4*	/	*0*	*1.2–1.5*	/	*100*
Marañon River	*18*	*15–69*	*<1–84*	*1*	*17*	*0.01–6.6*	*0.1*	*28*
Pastaza River	*5*	*25–40*	*<1–2*	*1*	*0*	*0.1–0.7*	*0.3*	*20*
Terra Firme	13	30–73	<1–4	1	0	0.01–0.31	0.1	0
Region B	23	17–62	<1–428	<1	9	<0.01–3.4	0.1	13
CDF	4	29–62	1–428	/	50	<0.01–0.4	/	25
LDF	1	28	<1	/	/	3.4	/	/
Terra Firme	18	17–43	<1–2	<1	0	<0.01–0.4	0.1	5
Region C	72	11–110	<1–114	<1	10	<0.01–4.4	0.03	26
CDF	4	16–60	2–114	/	50	0.4–1.7	/	100
LDF	19	11–96	<1–50	4	26	<0.01–4.4	0.7	74
Terra Firme	49	24–110	<1–2	<1	0	<0.01–2.0	0.01	4
Total	151	11–110	<1–428	1	18	<0.01–6.6	0.2	32
CDF	**28**	**15–96**	**<1–428**	**35**	**71**	**<0.01–5.4**	**0.8**	**71**
LDF	**43**	**12–69**	**<1–84**	**2**	**19**	**0.01–6.6**	**0.4**	**49**
Terra Firme	80	17–110	<1–4	<1	0	<0.01–2.0	0.02	4

in a sand-layer. On the LDF, organic-rich layers were observed in the riverbanks during our field campaign and described by well-owners. Their depth is estimated at around 18 and 30 m.

5.2. Hydrochemistry

5.2.1. Groundwater

Groundwater chemical parameters range from oxidizing and acidic to reducing and slightly alkaline. All arsenic-enriched groundwaters (>10 μg/L As) have a pH between 6.3 and 7.1 and are reducing, with an inverse correlation between Eh-field measurements and arsenic-concentrations (Fig. S.I.1a). A similar observation can be made for manganese-concentrations (Fig. S.I.1b). Contaminated groundwater is medium to highly ionized, with an electrical conductivity ranging from 260 to 1820 μS/cm (average and median 700 μS/cm).

The main ion-ratios vary substantially when considering the entire dataset (Fig. 4a). Arsenic-enriched groundwater falls within two compositions, either of the calcium-magnesium-bicarbonate-type (Zone I) or on a line with relatively constant calcium-magnesium ratios, with increasing sodium, and less dominant bicarbonate water (Zone II). Relating the hydrochemistry with the location of the wells within the river basin and taking into account the depth of the wells, these two compositional groups correspond to wells reaching aquifers within two specific parts of the river basins. Zone I corresponds to the aquifer(s) within the CDF, respectively Zone II to shallow aquifer(s) within the LDF. All arsenic-enriched groundwater tapped by wells located on the CDF are of the calcium-magnesium-bicarbonate type. Well-waters on LDF are grouped along relatively constant calcium numbers (Ca#: (Ca/Ca + Mg)) towards the sodium-corner and are slightly enriched in chloride and sulphate.

A similar distinction is illustrated in Fig. 4b, in which the ratio of Mg/Na versus Ca/Na is plotted. The wells of Zone I plot towards the upper-right corner, whereas the wells of Zone II are shifted towards the left of the graph. The increase in sodium relative to the bivalent cations indicates increased ion-exchange, hence chemically more evolved groundwater. The residue of the studied groundwater varies broadly.

Wells that are located on Terra Firme tap groundwater with a heterogeneous chemical composition that reflects the different geological formations in which the aquifers are embedded. Most groundwaters are characterized by an Eh superior to 200 mV, acidic pH between 4.0 and 6.2, rather low ionization and indicating chemically weathered aquifers. Interestingly, all the wells on the Madeira terrace are somewhat different, plotting towards enrichment of magnesium compared to calcium (Fig. 4b). This groundwater is oxidizing (Fig. 3c), less ionized (EC 10–100 μS/cm) and acidic (pH 4.4–5.8) (Table S.I.2). A minor part of the wells provides groundwater that is neutral to alkaline (pH 6.7–8.2), with typically lower Eh, between 0 and 200 mV. These wells are located within study region A either on the Terra Firme or are deeper wells located within the LDF. This groundwater is medium ionized (EC ~300–600 μS/cm) and of similar cation composition as the overlap between Zone I and Zone II.

5.2.2. Surface water

In all surface water samples arsenic-concentrations are ≤5 μg/L (Table S.I.2). Surface waters show a broad variety in cations, related to the type of river (Table S.I.2). Blackwater type rivers and lakes (e.g. the Negro and Nanay Rivers) are poorly ionized and of the (sodium + potassium) - bicarbonate-type, whereas the whitewater type rivers (e.g. the Amazon and Pastaza Rivers) are medium ionized and are of the calcium-bicarbonate type.

6. Discussion

6.1. Where -and where not- groundwater is prone to arsenic and manganese enrichment

Our results clearly demonstrate that mobilization and accumulation of arsenic and manganese take place in aquifers in the floodplains of the Amazon River and its main whitewater tributaries, both in the sub-Andean foreland basins, and in the floodplains further down-stream. The three investigated regions represent different structural parts of the river basins. Combining the results reveals a pattern, although the numbers of wells inside versus outside the floodplain are different in each study region (Table 1 and Fig. 5): 70 % of the wells on the most dynamic part of the floodplains (CDF) of whitewater rivers -that is the sediment-loaden rivers originating in the Andes- tap groundwater with arsenic concentrations above 10 μg/L, and manganese concentrations above 0.4 mg/L. Only 20 % of the wells on the less-dynamic part of these floodplains (LDF) have groundwater arsenic concentrations above 10 μg/L, while manganese concentrations exceed 0.4 mg/L in 50 % of the wells. Within this zone, only shallow wells are prone to arsenic contamination. None of the sampled wells on higher-lying areas outside of the actual floodplain of sediment-

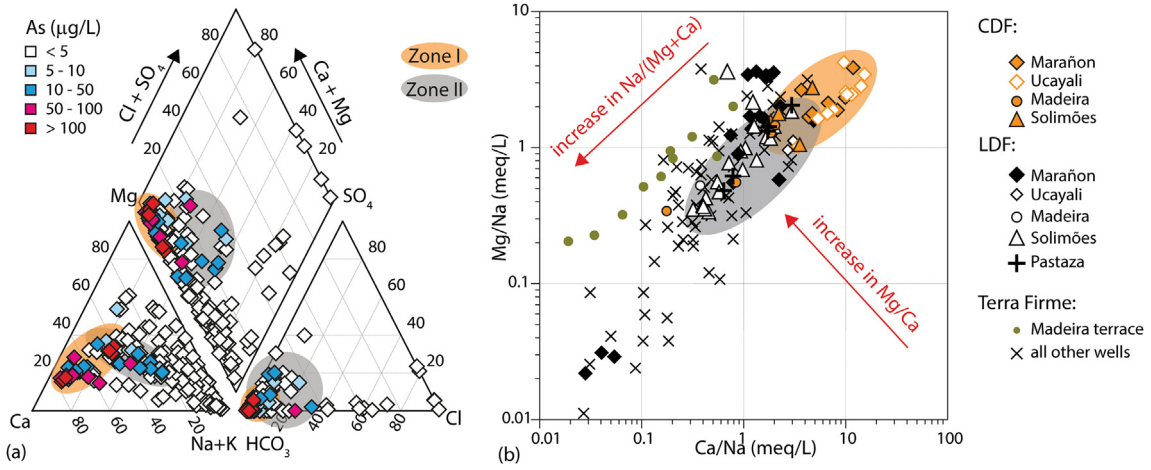

Fig. 4. Major ion composition of groundwaters from all three studied regions. (a) Piper diagram with the symbol coding related to the aqueous arsenic-concentration. Groundwaters enriched in arsenic are of two distinct major ion compositions, indicated as Zone I and Zone II. (b) Ca/Na versus Mg/Na binary plot with the symbol-coding in analogy to the location of the sampled well within the river basin. An increase in sodium relative to the sum of the bivalent cations (Ca + Mg) correlates with chemical evolution of the groundwater. Most waters from wells on the CDF fall into Zone I, whereas part of the wells on the LDF fall into Zone II. Groundwater in Zone I is generally more enriched in the bivalent cations (Ca + Mg) relative to sodium as in Zone II.

rich rivers, or on riverbanks of sediment-poor rivers exceeded 5 µg/L arsenic, respectively <5 % exceeded 0.4 mg/L manganese.

6.1.1. Arsenic and manganese enrichment in areas of recent/rapid sedimentation

Our spatial analysis permits the identification of two zones with aquifers at risk of groundwater arsenic and manganese enrichment within the floodplain, and the development of a conceptual model of arsenic accumulation (Fig. 6). The two zones are located within two distinct depositional environments of sediment-rich Andean (= whitewater) rivers. Aquifers with groundwater arsenic and manganese enrichment of concern are: (1) Zone I within the channel-dominated part of the floodplain (CDF) and (2) Zone II within the less-dynamic part of the floodplain (LDF).

In *Zone I* arsenic-rich groundwater is of the calcium-magnesium-bicarbonate type, reducing, near-neutral to slightly acidic and associated with elevated concentrations of aqueous iron and/or manganese, ammonium and DOC (Figs. 3 & 4). The dominant arsenic species is As^{III} (Table S.I.2). These hydrochemical groundwater characteristics in Zone I are consistent with arsenic-mobilization by microbially induced reductive dissolution of iron(hydr)oxides in fresh, un- or poorly altered sediments (Nickson et al., 1998; Smedley and Kinniburgh, 2002; Islam et al., 2004). Zone I consists of alluvial sediments, deposited and reworked by the rapidly moving river. The rapid burial of coarser grained sediments (which become aquifers) by organic-rich alternating silts and clays most likely favors the formation of strongly reducing conditions that enable the mobilization of the poorly bound arsenic. In the Amazonian floodplains, the total thickness of these deposits at risk is mostly unknown. Few geochronological data exist for these sediments. Exposed riverbanks are Holocene in age. Whether the entire Zone I consists of Holocene sediments or includes underlying older sediments, remains unknown. Within our studied area, deeper aquifers were only reached in the CDF of the Madeira River (study region B). The red hard layer at 33 m depth reported by the local population is most likely a paleosol, representing an unconformity between recent deposits of the Madeira channel and older deposits. Upstream of the study region A, along the Ucayali River in the Ucayali sub-Andean foreland basin, wells as deep as 80 m also tap older, arsenic-poor aquifers (de Meyer et al., 2017).

The few wells tapping groundwater with arsenic concentrations below 10 µg/L within Zone I are shallow (Fig. 3). Compared to the arsenic-enriched (>10 µg/L) groundwater in Zone I, the arsenic-poor groundwater features more sulfate, a more elevated Eh, and lower concentrations of ammonium. In the study region C these wells are in a sand layer not covered by fine-grained sediments (communication of well owners), both on point- and mid-channel bars. One hypothesis is that a significant infiltration of oxygen-rich surface water limits the achievement of reducing conditions in these shallow unconfined aquifers, at least during low-river stages.

Zone II corresponds to the shallow subsurface of the LDF. The upper part is formed by overbank deposits intercalated with peat layers. The groundwater in Zone II, enriched or not in groundwater arsenic and manganese, contains increasing sodium, chloride and sulfate, compared to groundwater of Zone I (Fig. 4a). The main cations are consistent with groundwater that underwent increased ion-exchange (Fig. 4b, Table S.I.2). The overbank deposits are seasonally exposed above the river level, inducing a water flow towards the river. The sediments were recently not re-worked, as these aquifers are located outside of the active part of the floodplain. The Eh, pH, DOC and ammonium are similar to groundwater from Zone I. The shallowest wells have mainly a higher Eh, higher sulfate and lower

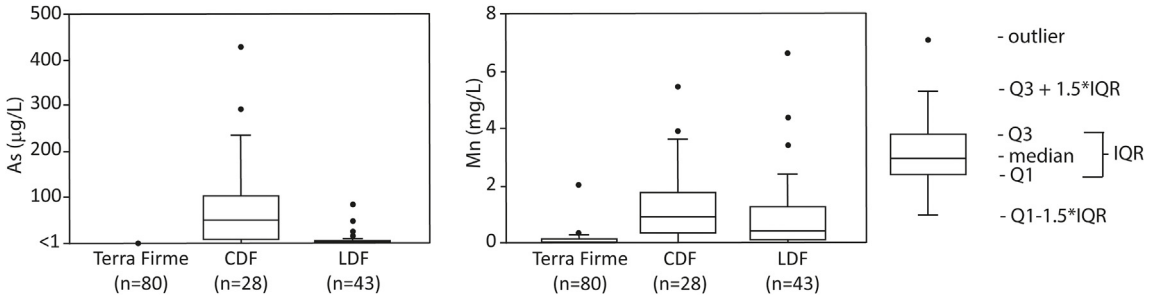

Fig. 5. Box and whisker plots of the arsenic and manganese concentrations of wells on the different structural parts of the floodplains, i.e. the channel-dominated part of the floodplain (CDF) and the less-dynamic part of the floodplain (LDF), versus the Terra Firme.

ammonium concentrations. The conditions are thus likely not sufficiently reducing for aqueous arsenic accumulation. The shallowest wells are in between high and low stands of the seasonal groundwater table, with the wells drying out at the end of the dry season. The observed variability in arsenic concentrations of groundwaters in Zone II might be related to the presence of the black peat layers, whether as a pool for reactive organic matter, or as a sink/source for arsenic, with the formation of sulfide phases (e.g. Burton et al., 2014). Water of some of the wells within Zone II had a strong sulfur smell, an indication of sulfate reduction to H_2S. In some groundwaters of Zone II, As^{III} corresponds to only 50 % of total arsenic (Table S.I.2), which is likely caused by an interplay of oxidation and reduction, or even mixing of water in a heterogeneous aquifer.

The peat layers within Zone II are Holocene in age (see chapter 4). For deeper sediments age determinations are rare. Along the Solimões River (study region C), the deepest dated sediments are located at the base of the riverbanks. In some places of the LDF along the Solimões River a few meters below the Holocene organic-rich layers, a late-Pleistocene age has been determined for the sediments (Latrubesse and Franzinelli, 2002; Passos et al., 2020). This part of the floodplain is only partially affected by flooding, with very little sediments from the Solimões River being deposited (Latrubesse and Franzinelli, 2002). As such, the aquifers in Zone II might have been prone to stronger chemical weathering, with stabilization of the manganese and iron-phases and organic carbon (see chapter 6.2).

6.1.2. Absence of arsenic enrichment related to absence of young alluvial aquifers

Outside of these two zones at risk, no arsenic contaminated groundwater was encountered (Table 1). All other wells are either located on the terraces outside of the modern floodplains of whitewater rivers, here grouped as Terra Firme, or within these floodplains, but reaching aquifers below the zones at risk of both LDF and CDF (conceptual illustration Fig. 6). Our results are consistent with former groundwater studies in towns located on Terra Firme along the Amazon River (CPRM, 2009) upstream of our study region C, where arsenic-concentrations were always below 8 μg/L (LOQ of the studies).

The characteristics of the Terra Firme well-water points to an absence of subsurface conditions allowing for groundwater arsenic accumulation. The sediments of the aquifers are mainly matured and oxidized sands, leading to oxidizing aquifer conditions. In the aquifers with reducing, alkaline groundwater tapped by few wells on Terra Firme (Table S.I.2), arsenic could be bound in sulfide minerals, a hypothesis that awaits further study.

The Madeira terrace is a relatively young formation of the Madeira River (study region B) with paleorias filled with a 9 m thick layer of clay (Bertani et al., 2015). Below this clay, a fining upward sequence of yellow-reddish sandstones and brown to grey mudstones occur (Bertani et al., 2015; Rossetti et al., 2014). Organic-rich layers in the mudstones are Holocene in age in the upper part, and of late-Pleistocene age in the lower part (^{14}C-age determinations, Bertani et al., 2015). Although the upper sediments are fine-grained and recent, the aquifer below consists of older oxidized sediments. This could indicate recharge of the underlying aquifer outside of the paleorias with oxygen-rich water. Hence, the wells between 12 and 48 m depth are reaching the sand layers of late-Pleistocene age or older, below the Holocene paleoria infill. These aquifers are mostly highly oxidized and weathered. The similarity in results between wells on the paleoria and outside suggests that the thick Holocene clay pack currently does not influence arsenic-mobilization in the aquifer below. The iron-rich hard layers identified in previous studies (Bertani et al., 2015; Rossetti et al., 2014) may serve as a barrier for arsenic-mobilization from the young clay-layers. There is also no difference in hydrochemistry between wells on the Madeira terrace and the wells on other parts of the Terra Firme within the study region B.

The Terra Firme terrains are drained by blackwater streams. As a consequence, wells on the riverbanks of blackwater rivers are tapping similar aquifers as Terra Firme riverbanks along the whitewater rivers. In the floodplains of blackwater rivers, current supply of chemically poorly weathered sediments in quantities allowing for the formation of reducing aquifers is missing. Some shallow wells tap aquifers in the upper sediments that can consist of pure white sands, resulting in very acidic (pH < 4.5) and oxygenated water, mobilizing aluminum, as it is the case in wells around Manaus (in study region C) (see Table S.I.2), and is similar as described in de Meyer et al. (2017).

We conclude that groundwater arsenic enrichment is related to recent sediment accumulation at high rates. Such areas allow to form aquifers in which arsenic and manganese can easily mobilize and accumulate. The inverse, areas with low sedimentation and/or with little accumulation are unlikely to host aquifers at risk of arsenic groundwater contamination. Where conditions of iron and manganese oxide dissolution are reached, however, groundwater iron and manganese concentrations above the drinking water guideline values do occur. It remains open how vulnerable shallow aquifers in Terra Firme are to arsenic mobilization by anthropogenic induced groundwater flow from the riverside inland, as documented e.g. by Wallis et al. (2020) near the city of Hanoi in Vietnam.

6.2. As versus Mn and Fe mobilization

Within the floodplains, both zones at risk for groundwater arsenic accumulation are also enriched in manganese. A scattering in arsenic versus manganese concentrations is observed (Fig. 7a), and groundwater elevated in both manganese and arsenic does occur. However, arsenic enrichment only takes place where the aqueous Mn/Fe ratio is below 1 (Fig. 7b).

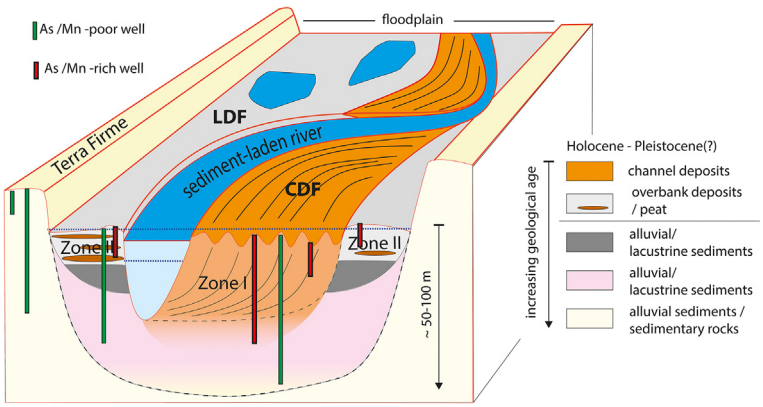

Fig. 6. Conceptual illustration: sketch of a typical Amazonian floodplain of a sediment-laden river (Andean - whitewater river). Not on scale - vertically exaggerated. In reality, the alluvial sedimentary basin has a complex 3 D architecture, that will be different for each study region. The floodplain can be divided in two main parts: the dynamic part of the floodplain, under influence of the river channeling - channel-dominated floodplain (CDF), and that part of the floodplain, outside of the influence of the river channel, less-dynamic floodplain (LDF). Aquifers at risk for arsenic and manganese groundwater contamination are located within the floodplain.

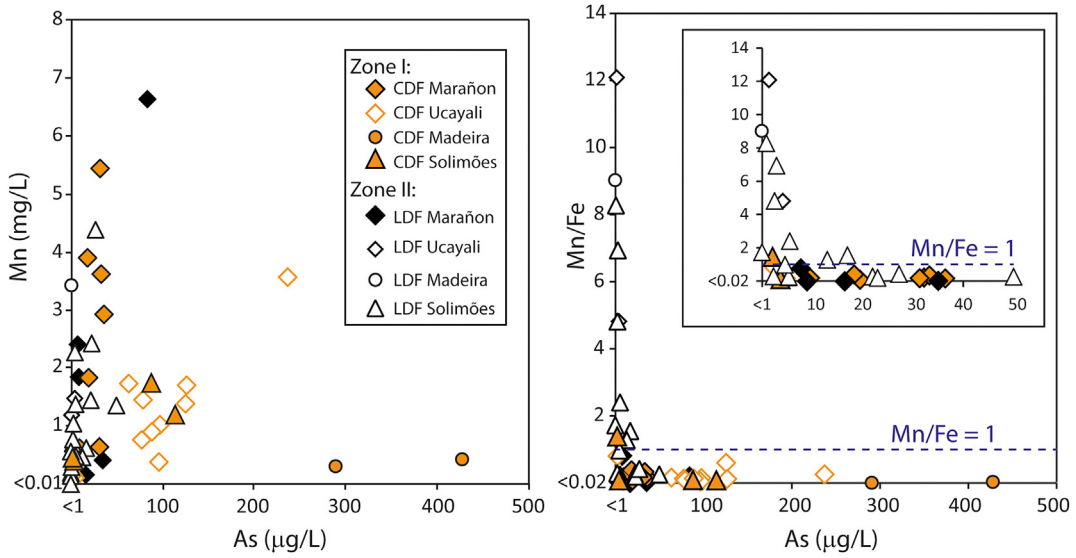

Fig. 7. Groundwater Mn versus As and the Mn/Fe-ratio versus As - concentrations for wells located on the floodplains of the Andean rivers. The wells clearly reaching deeper deposits, hence below Zone I and Zone II, are not on the chart. Simultaneous elevated concentrations of manganese and arsenic are excluded if not accompanied with elevated concentrations of iron. Water with concurrent elevated concentrations in manganese, arsenic and iron, however, does occur.

Hence, our results indicate that coupled arsenic and manganese enrichment is only occurring with simultaneous iron enrichment, in agreement with the proposed concept that the relation between arsenic, manganese, and iron concentrations depends upon the degree of completion of iron(hydr)oxide reduction and of buffering with manganese oxides (McArthur et al., 2004; Buschmann et al., 2007; McArthur et al., 2012). For example, along the Madeira River (study region B) the arsenic-enriched groundwater in Zone I has manganese concentrations below 1 mg/L but is enriched in iron (Figs. 3b & 7b), indicating advanced iron reduction. A contrasting behavior is observed in the Ucamara depression (study region A) between the floodplains of the Marañon versus the Ucayali River (Fig. 2a). Along the Ucayali river, wells within Zone I tap water above 50 µg/L arsenic, whereas along the Marañon it is between 10 and 50 µg/L arsenic. The concentrations in main cations do not differ significantly (Fig. 4b). At the same time the arsenic versus manganese concentrations for wells in Zone I of the Marañon River (study region A) and in Zone II of the Solimões River (study region C) plot similar, whereas the wells of Zone I of the Ucayali River (study region A) behave like the wells in Zone I of the Solimões River (Fig. 7a). But the groundwater along the Marañon River is more enriched in both manganese and iron, hence, iron reduction and manganese reduction are coeval. In contrast, only manganese-reduction takes place in the arsenic poor groundwater in Zone II of the LDF and in some shallow wells of the channel-dominated floodplains.

6.3. The role of fluvial dynamics

As any further information on the aquifer characteristics (stratigraphy, mineralogy, burial age, etc.) is not available, we currently only consider the fluvial dynamics to explain the observed variability within the floodplains. In our study area, the Marañon River is anabranching, with a small and non-continuous channel-dominated floodplain, whereas the Ucayali River is meandering within a significantly larger, continuous floodplain (Fig. 2a). This difference is likely related to a lower slope for the Ucayali River and may also be influenced by the northward migration of the Marañon River, thereby blocked by the Pastaza fan sediments (Dumont, 1991; Räsänen et al., 1992). The actual channel is presumably quite young (Lähteenoja et al., 2012), whereas the Ucayali River is dominantly moving inside its broad channeling, that could imply ongoing reworking of sediments through rapid channel migration (Kalliola et al., 1992).

The origin of aqueous arsenic and the according controlling factors are debated. The consensus on the origin of arsenic release in the severely affected and intensively studied aquifers in South and South East Asia is that arsenic is mainly released in young Holocene sediments. In that zone, both reactive organic carbon and reactive iron(hydr)oxide phases with absorbed arsenic are abundant. Seasonally deposited fresh sediments offer new sources of these reactive substances. Downward flow of groundwater can transport aqueous arsenic or reactive organic matter to deeper aquifers (Kocar et al., 2008; Polizzotto et al., 2008; Winkel et al., 2011; Stuckey et al., 2016). Availability and reactivity of organic matter as a driver for redox-reactions plays a crucial role (Lovley, 1995; Nickson et al., 2000; McArthur et al., 2004; Meharg et al., 2006; Glodowska et al., 2020). This implies that local heterogeneities of the aquifers in organic matter supply and hydraulic conductivity controls the spatial variability in aqueous arsenic-concentrations (McArthur et al., 2004; Papacostas et al., 2008; Donselaar et al., 2017; Magnone et al., 2017; Stopelli et al., 2021; Lightfoot et al., 2022). Recent studies in South and Southeast Asia advanced the idea that the most dynamic parts of floodplains and delta's including meandering belts and active floodplain, are most prone for arsenic contamination (e.g. Das and Mondal, 2021 in Bengal; Kazmierczak et al., 2022 Red River in Vietnam; Magnone et al., 2017 Mekong River in Cambodia). Hence, the Amazonian floodplains and its arsenic and manganese distribution follows a similar pattern that can be observed globally in affected river basins and deltas. This observation favors a general model that arsenic and manganese distribution is globally controlled by the depositional dynamics of river systems.

We propose that the interplay of burial rate, drainage, depth of sediment reworking and mineral proportions reflect fluvial dynamic processes that determine the mobilization of arsenic and manganese in shallow aquifers of the studied Amazonian floodplains. To determine the main controlling factor, a detailed comparison of the stratigraphy and aquifer chemistry along the various rivers in lowland Amazonia is required.

7. Conclusions and outlook

Basin-wide arsenic contamination of groundwater resources in Amazonia is observed in specific parts of the active Andean river floodplains. Based on satellite images, the vulnerable areas can be delineated in its structural geometry. Arsenic and manganese is mobilized in the aquifers of channel-dominated parts of the floodplains of sediment-laden Andean

rivers. In the less active parts of the floodplains, further mobilization does occur in overbank deposits or in organic-rich layers.

Larger towns and cities are mainly built on Terra Firme (with exceptions in the Andean foreland basins), where this study showed that the risk for natural arsenic and manganese groundwater contamination can be considered as low. However, the rural population living on the riverbanks within the floodplain of the Amazon River and its main whitewater tributaries is exposed to the threat of arsenic and manganese in its groundwater resources.

Our study emphasizes that a thorough understanding of the dynamics and morphological evolution of the river systems in the search for contaminant-free groundwater is needed. With the increasing societal demand for clean water, it is key to identify areas of uncontaminated aquifers and how vulnerable these are for future arsenic mobilization. Hence, combined in-depth hydrogeological and stratigraphic investigations of the region are required. Deciphering the groundwater flow and recharge, and their relations with sedimentary stratigraphy will be essential to clarify the causes of the differences between the floodplains observed in our study.

The aquifers of the Amazon River floodplains follow the commonly accepted concepts of arsenic mobilization in reducing groundwater. An advantage of lowland Amazonia is the relatively low population-, and subsequent well-density, giving place for investigating the controlling processes in natural systems. We emphasize that other arsenic mobilization mechanism may occur in mineralized areas on the cratons, or in the drier southern parts of the Amazon.

Supplementary data to this article can be found online at https://doi.org/10.1016/j.scitotenv.2022.160407.

Data availability

The complete set of hydrochemical data presented in this publication is available in the supplementary table: Table SI.2.

Declaration of competing interest

The authors declare that they have no known competing financial interests or personal relationships that could have appeared to influence the work reported in this paper.

Acknowledgements

The authors would like to thank all the well owners for giving access to their wells and for their hospitality. The AuA-team at Eawag, Thomas Rüttimann, Caroline Stengel and Numa Pfenninger are acknowledged for chemical analysis of the water samples. We are grateful to Patricia Roeser and to the students from UFAM Manaus, João Matheus, Lucindo Antunes Fernandes Neto, Thaynara Sampaio Brito, and Julio Iago Bailosa Silva, as well as Amazonino Lemos de Castro, Keith Soares Valente (UFAM Humaitá) for their assistance during field campaigns in the Brazilian Amazon. Special thanks to Toto and the boat crew from Comandante Gomes III, as well as Camila Ribas and the INPA-team, each of whom highly contributed to the success and fascinating atmosphere of the Solimões expedition. We would like to thank in the same way our boat drivers (Alex Cassanza Cassaza and Luis Goncales Vasquez) and guide (Luis Alberto López Ramirez), whose expertise considerably contributed to the achievement of the Peruvian expedition.

CdM and MB gratefully acknowledge the research grant of the Swiss National Science Foundation (SNSF grant 200021-165913), seed money of the Latin America - Swiss Bilateral Programme (CODEV-EPFL) (SM-LA 21), as well as seed money of the Brazilian Swiss Joint Research Programme (BSJRP). IW received financial support of the Brazilian Federal Research Council (CNPq) (Project grant 433203/2016-1). EACD would like to thank the Peruvian National Fund for Scientific and Technological Development for scholarship (Project contract No. 05-2018-FONDECYT/BM). We thank Jagannath Biswakarma for comments on an earlier version and Peter Knappett and two anonymous reviewers for their constructive comments.

References

Aalto, R., Dunne, T., Guyot, J.L., 2006. Geomorphic controls on Andean denudation rates. J. Geol. 114, 85–99.

Acharyya, S.K., Lahiri, S., Raymahashay, B.C., Bhowmik, A., 2000. Arsenic toxicity of groundwater in parts of the Bengal basin in India and Bangladesh: the role of Quaternary stratigraphy and Holocene sea-level fluctuation. Environ. Geol. 39 (10), 1127–1137.

Acharyya, S.K., Shah, B.A., 2007. Arsenic-contaminated groundwater from parts of Damodar fan-delta and west of Bhagirathi River, West Bengal, India: influence of fluvial geomorphology and Quaternary morphostratigraphy. Environ. Geol. 52, 489–501.

Bahia, R.B.C., Oliveira, M.A., 2004. Folha SB20-Purus. In: Schobbenhaus, C., Gonçalves, J.H., Santos, J.O.S., Abram, M.B., Leão Neto, R., Matos, G.M.M., Vidotti, R.M., Ramos, M.A.B., Jesus, J.D.A. de (Eds.), Carta Geológica do Brasil ao Milionésimo, Sistema de Informações Geográficas. Programa Geologia do Brasil. CPRM, Brasília CD-ROM.

Berg, M., Trang, P.T.K., Stengel, C., Buschmann, J., Viet, P.H., Van Dan, N., Giger, W., Stüben, D., 2008. Hydrological and sedimentary controls leading to arsenic contamination of groundwater in the Hanoi area, Vietnam: the impact of iron-arsenic ratios, peat, river bank deposits, and excessive groundwater abstraction. Chem. Geol. 249 (1–2), 91–112.

Bernal, C., Christophoul, F., Darrozes, J., Soula, J.C., Baby, P., Burgos, J., 2011. Late glacial and Holocene avulsions of the Rio Pastaza Megafan (Ecuador-Peru): frequency and controlling factors. Int. J. Earth Sci. 100, 1759–1782.

Bertani, T.C., Rossetti, D.F., Hayakawa, E.H., Cohen, M.C.L., 2015. Understanding Amazonian fluvial rias based on a Late Pleistocene-Holocene analog. Earth Surf. Process. Landf. 40, 285–292.

Bezerra, I.S.A.A., Nogueira, A.C.R., Motta, M.B., Sawakuchi, A.O., Mineli, T.D., Silva, A.Q., Silva Jr., A.G., Domingos, F.H.G., Mata, G.A.T., Lima, F.J., Riker, S.L.R., 2022. Incision and aggradation phases of the Amazon River in central-eastern Amazonia during the Late Neogene and Quaternary. Geomorphology 399, 108073. https://doi.org/10.1016/j.geomorph.2021.108073.

Bundschuh, J., Niazi, N.K., Alam, M.A., Berg, M., Herath, I., Tomaszewska, B., Maity, J.P., Ok, Y.S., 2022. Global arsenic dilemma and sustainability. J. Hazard. Mater. 436, 129197. https://doi.org/10.1016/j.jhazmat.2022.129197.

Burton, E.D., Johnston, S.G., Kocar, B.D., 2014. Arsenic mobility during flooding of contaminated soil: the effect of microbial sulfate reduction. Environ. Sci. Technol. 48, 13660–13667.

Buschmann, J., Berg, M., Stengel, C., Sampson, M.L., 2007. Arsenic and manganese contamination of drinking water resources in Cambodia: coincidence of risk areas with low relief topography. Environ. Sci. Technol. 41, 2146–2152.

CPRM, 2009. Avaliação das águas de abastecimento público, da destinação dos residuos sólidos, das áreas de risco geológico e dos insumos minerais para construção civil nas sedes do municipios situados na região do Alto Solimões (AM). CPRM, Manaus 448pp.

Das, A., Mondal, S., 2021. Geomorphic controls on shallow groundwater arsenic contamination in Bengal basin, India. Environ. Sci. Pollut. Res. 28, 42177–42195.

De La Cruz, N., Zuolaga, A., Geldres, M., Fidel, L., Cavaro, R., Hipólito, A., Lipa, V., Ticona, P., Valdivia, W., 1999. Geología de los cuadrángulos 11-l, 11-m, 12-l, 12-m, 11-n, 11-ñ, 11-o, 11-p, 11-q, 12-n, 12-ñ, 12-o, 12-p, 12-q, 13-ñ, 14-ñ, 13-o, 14-o,13-p y 14p. INGEMMET, Boletín, Serie A 134, 255.

de Meyer, C.M.C., Rodriguez, J.M., Carpio, E.A., Garcia, P.A., Stengel, C., Berg, M., 2017. Arsenic, manganese and aluminum contamination in groundwater resources of Western Amazonia (Peru). Sci. Total Environ. 607, 1437–1450.

Donselaar, M.E., Bhatt, A.G., Ghosh, A.K., 2017. On the relation between fluvio-deltaic flood basin geomorphology and the wide-spread occurrence of arsenic pollution in shallow aquifers. Sci. Total Environ. 574, 901–913.

Dumont, J.-F., 1991. Fluvial shifting in the Ucamara Depression as related to the neotectonics of the Andean foreland Brazilian Craton Border (Peru). Géodynamique 6, 9–20.

Dumont, J.F., 1996. Neotectonics of the Subandes-Brazilian craton boundary using geomorphological data: the Maranon and Beni Basins. Tectonophysics 259, 137–151.

Dumont, J.F., Fournier, M., 1994. Geodynamic environment of quaternary morphostructures of the subandean foreland basins of Peru and Bolivia: characteristics and study methods. Quat.Int. 21.

Dumont, J.F., Garcia, F., 1991. Active subsidence controlled by basement structures in the Marañon basin of Northeastern Peru., Land subsidence. Proceedings of the Fourth International Symposium of Land Subsidence, pp. 343–350 (579 p).

Dumont, J.F., Lamotte, S., Fournier, M., 1988. Neotectonico del arco de Iquitos (Jenaro Herrera, Peru). Bol. Soc. Geol. Perú 77, 7–17.

Dunne, T., Mertes, L.A.K., Meade, R.H., Richey, J.E., Forsberg, B.R., 1998. Exchanges of sediment between the flood plain and channel of the Amazon River in Brazil. Geol. Soc. Am. Bull. 110, 450–467.

Erban, L.E., Gorelick, S.M., Zebker, H.A., Fendorf, S., 2013. Release of arsenic to deep groundwater in the Mekong Delta, Vietnam, linked to pumping-induced land subsidence. Proc. Natl. Acad. Sci. U. S. A. 110, 13751–13756.

Espinoza Villar, J.C., Ronchail, J., Guyot, J.L., Cochonneau, G., Naziano, F., Lavado, W., De Oliveira, E., Pombosa, R., Vauchel, P., 2009. Spatio-temporal rainfall variability in the Amazon Basin countries (Brazil, Peru, Bolivia, Colombia, and Ecuador). Int. J. Climatol. 29, 1574–1594. https://doi.org/10.1002/joc.1791.

FAO, 2015. AQUASTAT Transboundary River Basin Overview – Amazon. Food and Agriculture Organization of the United Nations (FAO), Rome, Italy.

Faria, M.S.G., Bahia, R., Almeida, M.E., Oliveira, M.A., 2004. Folha SA.20-Manaus. In: Schobbenhaus, C., Gonçalves, J.H., Santos, J.O.S., Abram, M.B., Leão Neto, R., Matos, G.M.M., Vidotti, R.M., Ramos, M.A.B., Jesus, J.D.A. de (Eds.), Carta Geológica do Brasil ao Milionésimo, Sistemas de Informações Geográficas-SIG. Programa Geologia do Brasil, CPRM, Brasília CD-ROM.

Filizola, N., Guyot, J.L., 2009. Suspended sediment yields in the Amazon basin: an assessment using the Brazilian national data set. Hydrol. Process. 23, 3207–3215. https://doi.org/10.1002/hyp.7394.

Filizola, N., Guyot, J.-L., Wittmann, J.H.Martinez, Oliveira, E., 2011. The significance of suspended sediment transport determination on the amazonian hydrological scenario. In: Manning, A.J. (Ed.), Sediment Transport in Aquatic Environments. IntechOpen, pp. 45–64 https://doi.org/10.5772/19948.

Frisbie, S.H., Mitchell, E.J., Dustin, H., Maynard, D.M., Sarkar, B., 2012. World Health Organization discontinues its drinking-water guideline for manganese. Environ. Health Perspect. 120 (6), 775–778.

Gibbs, R.J., 1967. The geochemistry of the Amazon River system: part I. The factors that control the salinity and the composition and concentration of the suspended solids. Geol. Soc. Am. Bull. 78, 1203–1232.

Glodowska, M., Stopelli, E., Schneider, M., Lightfoot, A., Rathi, B., Straub, D., Patzner, M., Duyen, V.T., Members, AdvectAs Team, Berg, M., Kleindienst, S., Kappler, A., 2020. Role of in situ natural organic matter in mobilizing as during microbial reduction of FeIII-mineral-bearing aquifer sediments from Hanoi (Vietnam). Environ. Sci. Technol. 54, 4149–4159. https://doi.org/10.1021/acs.est.9b07183.

Gonçalves Júnior, E.S., Soares, E.A.A., Tatumi, S.H., Yee, M., Mittani, J.C.R., 2016. Pleistocene-Holocene sedimentation of solimoes-Amazon fluvial system between the tributaries Negro and Madeira, Central Amazon. Braz. J. Geol. 46, 167–180.

Guyot, J.L., 1993. Hydrogéochimie des fleuves de l'Amazonie bolivienne. ORSTOM, Paris 261 pp.

Guzmán, A., Zavala, B., Aldana, M., 1999. Geología de los cuadrángulos 13-m y 14-m. INGEMMET, Boletín Serie A 92 Lima, 133 pp.

Harvey, C.F., Swartz, C.H., Badruzzaman, A.B.M., Keon-Blute, N., Yu, W., Ali, M.A., Jay, J., Beckie, R., Niedan, V., Brabander, D., Oates, P.M., Ashfaque, K.N., Islam, S., Hemond, H.F., Ahmed, M.F., 2002. Arsenic mobility and groundwater extraction in Bangladesh. Science 298, 1602–1606.

Hayakawa, E.H., Rossetti, D.F., 2015. Late quaternary dynamics in the Madeira river basin, southern Amazonia (Brazil), as revealed by paleomorphological analysis. An. Acad. Bras. Cienc. 87, 29–49.

Hoorn, C., Wesselingh, F.P., ter Steege, H., Bermudez, M.A., Mora, A., Sevink, J., Sanmartin, I., Sanchez-Meseguer, A., Anderson, C.L., Figueiredo, J.P., Jaramillo, C., Riff, D., Negri, F.R., Hooghiemstra, H., Lundberg, J., Stadler, T., Sarkinen, T., Antonelli, A., 2010. Amazonia through time: Andean uplift, climate change, landscape evolution, and biodiversity. Science 330, 927–931.

INGEMMET, 1999. Carta Geológica Nacional. Escala 1:100.000 Lima, Peru.

INGEMMET, 2016. Carta Geológica Nacional. Escala 1:100.000. Versión digital estandardizada Lima, Peru.

Islam, F.S., Gault, A.G., Boothman, C., Polya, D.A., Charnock, J.M., Chatterjee, D., Lloyd, J.R., 2004. Role of metal-reducing bacteria in arsenic release from Bengal delta sediments. Nature 430, 68–71.

Jakobsen, R., Kazmierczak, J., Sø, H.U., Postma, D., 2018. Spatial variability of groundwater arsenic concentration as controlled by hydrogeology: conceptual analysis using 2-D reactive transport modeling. Water Resour. Res. 54, 10254–10269.

Junk, W.J., Piedade, M.T.F., Schongart, J., Cohn-Haft, M., Adeney, J.M., Wittmann, F., 2011. A classification of major naturally-occurring Amazonian lowland wetlands. Wetlands 31, 623–640.

Kalliola, R., Salo, J., Puhakka, M., Rajasilta, M., Hame, T., Neller, R.J., Rasanen, M.E., Arias, W.A.D., 1992. Upper Amazon channel migration – implications for vegetation perturbance and succession using bitemporal Landsat MSS Images. Naturwissenschaften 79, 75–79.

Kapaj, S., Peterson, H., Liber, K., Bhattacharya, P., 2006. Human health effects from chronic arsenic poisoning – a review. J. Environ. Sci. Health A 41, 2399–2428.

Kazmierczak, J., Postma, D., Dang, T., Van Hoang, H., Larsen, F., Hass, A.E., Hoffmann, A.H., Fensholt, R., Pham, N.Q., Jakobsen, R., 2022. Groundwater arsenic content related to the sedimentology and stratigraphy of the Red River delta, Vietnam. Sci. Total Environ. 814.

Kocar, B.D., Polizzotto, M.L., Benner, S.G., Ying, S.C., Ung, M., Ouch, K., Samreth, S., Suy, B., Phan, K., Sampson, M., Fendorf, S., 2008. Integrated biogeochemical and hydrologic processes driving arsenic release from shallow sediments to groundwaters of the Mekong delta. Appl. Geochem. 23, 3059–3071.

Kullar, S.S., Shao, K., Surette, C., Foucher, D., Mergler, D., Cormier, P., Bellinger, D.C., Barbeau, B., Sauvé, S., Bouchard, M.F., 2019. A benchmark concentration analysis for manganese in drinking water and IQ deficits in children. Environ. Int. 130.

Lähteenoja, O., Page, S., 2011. High diversity of tropical peatland ecosystem types in the Pastaza-Maranon basin, Peruvian Amazonia. J. Geophys. Res.Biogeosci. 116, 14.

Lähteenoja, O., Reategui, Y.R., Rasanen, M., Torres, D.D., Oinonen, M., Page, S., 2012. The large Amazonian peatland carbon sink in the subsiding Pastaza-Maranon foreland basin,Peru. Glob. Chang. Biol. 18, 164–178.

Latrubesse, E.M., Franzinelli, E., 2002. The Holocene alluvial plain of the middle Amazon River, Brazil. Geomorphology 44, 241–257.

Latrubesse, E.M., Restrepo, J.D., 2014. Sediment yield along the Andes: continental budget, regional variations, and comparisons with other basins from orogenic mountain belts. Geomorphology 216, 225–233.

Latrubesse, E.M., Cozzuol, M., da Silva-Caminha, S.A.F., Rigsby, C.A., Absy, M.L., Jaramillo, C., 2010. The Late Miocene paleogeography of the Amazon Basin and the evolution of the Amazon River system. Earth Sci. Rev. (ISSN: 0012-8252) 99 (3–4), 99–124. https://doi.org/10.1016/j.earscirev.2010.02.005.

Leite, N.K., Krusche, A.V., Ballester, M.V.R., Victoria, R.L., Richey, J.E., Gomes, B.M., 2011. Intra and interannual variability in the Madeira River water chemistry and sediment load. Biogeochemistry 105, 37–51.

Lightfoot, A.K., Brennwald, M.S., Prommer, H., Stopelli, E., Berg, M., Glodowska, M., Schneider, M., Kipfer, R., 2022. Noble gas constraints on the fate of arsenic in groundwater. Water Res. 214, 118199. https://doi.org/10.1016/j.watres.2022.118199.

Lombardo, U., 2014. Neotectonics, flooding patterns and landscape evolution in southern Amazonia. Earth Surf. Dyn. 2, 493–511.

Lovley, D.R., 1995. Microbial reduction of iron, manganese, and other metals. Adv. Agron. 54 (54), 175–231.

Magnone, D., Richards, L.A., Polya, D.A., Bryant, C., Jones, M., van Dongen, B.E., 2017. Biomarker-indicated extent of oxidation of plant-derived organic carbon (OC) in relation to geomorphology in an arsenic contaminated holocene aquifer,Cambodia. Sci. Rep. 7, 13093. https://doi.org/10.1038/s41598-017-13354-8.

Martínez, W., Morales, M., Díaz, G., Milla, D., Montoya, C., Huayhua, J., Romero, L., Raymundo, T., 1999. Geología de los cuadrángulos 5-n, 5-ñ, 5-o, 6-n, 6-ñ, 6-o, 7-n,7-ñ, 7-o, 8-n, 8-ñ, 8-o, 9-n, 9-ñ, 9-o, 10-n, 10-ñ y 10-o. INGEMMET, Boletín Serie A 131, 354.

McArthur, J.M., Banerjee, D.M., Hudson-Edwards, K.A., Mishra, R., Purohit, R., Ravenscroft, P., Cronin, A., Howarth, R.J., Chatterjee, A., Talukder, T., Lowry, D., Houghton, S., Chadha, D.K., 2004. Natural organic matter in sedimentary basins and its relation to arsenic in anoxic ground water: the example of West Bengal and its worldwide implications. Appl. Geochem. 19, 1255–1293.

McArthur, J.M., Nath, B., Banerjee, D.M., Purohit, R., Grassineau, N., 2011. Palaeosol control on groundwater flow and pollutant distribution: the example of arsenic. Environ. Sci. Technol. 45, 1376–1383. https://doi.org/10.1021/es1032376.

McArthur, J.M., Sikdar, P.K., Nath, B., Grassineau, N., Marshall, J.D., Banerjee, D.M., 2012. Sedimentological control on Mn, and other trace elements, in groundwater of the Bengal Delta. Environ. Sci. Technol. 46, 669–676.

McClain, M.E., Elsenbeer, 2001. Terrestrial inputs to Amazon streams and internal biogeochemical processing. In: McClain, M.E., Victoria, R.L., Richie, J.E. (Eds.), The Biogeochemistry of the Amazon Basin. Oxford University Press, New York, pp. 185–208.

Meade, R.H., Dunne, T., Richey, J.E., Santos, U.M., Salati, E., 1985. Storage and remobilization of suspended sediment in the lower Amazon River of Brazil. Science 228, 488–490.

Meharg, A.A., Scrimgeour, C., Hossain, S.A., Fuller, K., Cruickshank, K., Williams, P.N., Kinniburgh, D.G., 2006. Codeposition of organic carbon and arsenic in Bengal delta aquifers. Environ. Sci. Technol. 40, 4928–4935. https://doi.org/10.1021/es060722b.

Meng, X., Wang, W., 2008. Speciation of arsenic by disposable cartridges. Proceedings of the Third International Conference on Arsenic Exposure and Health Effects, Soc. Environ. Geochem. and Health. University of Colorado, Denver.

Mertes, L.A.K., Daniel, D.L., Melack, J.M., Nelson, B., Martinelli, L.A., Forsberg, B.R., 1995. Spatial patterns of hydrology, geomorphology, and vegetation on the floodplain of the Amazon river in Brazil from a remote-sensing perspective. Geomorphology 13, 215–232.

Mertes, L.A.K., Dunne, T., Martinelli, L.A., 1996. Channel-floodplain geomorphology along the Solimoes-Amazon River,Brazil. Geol. Soc. Am. Bull. 108, 1089–1107.

Mertes, L.A., Dunne, T., 2007. Effects of tectonism, climate change, and sea-level change on the form and behaviour of the modern Amazon River and its floodplain. In: Gupta, A. (Ed.), Large Rivers: Geomorphology and Management. John Wiley & Sons, pp. 115–144 https://doi.org/10.1002/9780470723722.ch8.

Mitchell, E.J., Frisbie, S.H., Roudeau, S., Carmona, A., Ortega, R., 2021. How much manganese is safe for infants? A review of the scientific basis of intake guidelines and regulations relevant to the manganese content of infant formulas. J. Trace Elem. Med. Biol. 65.

Mora, A., Baby, P., Roddaz, M., Parra, M., Christophoul, F., Brusset, S., Hermoza, W., Espurt, N., 2010. Tectonic history of the Andes and sub-Andean zones: implications for the development of the Amazon drainage basin. In: Hoorn, C., Wesselingh, F.P. (Eds.), Amazonia: Landscape & Species Evolution: A Look Into the Past. Blackwell Publishing Ltd, West Sussex, pp. 38–60.

Nath, B., Berner, Z., Chatterjee, D., Mallik, S.B., Stuben, D., 2008. Mobility of arsenic in West Bengal aquifers conducting low and high groundwater arsenic. Part II: comparative geochemical profile and leaching study. Appl. Geochem. 23, 996–1011.

Nickson, R.T., McArthur, J.M., Burgess, W., Ahmed, K.M., Ravenscroft, P., Rahman, M., 1998. Arsenic poisoning of Bangladesh groundwater. Nature 395, 338.

Nickson, R.T., McArthur, J.M., Ravenscroft, P., Burgess, W.G., Ahmed, K.M., 2000. Mechanism of arsenic release to groundwater, Bangladesh and West Bengal. Appl. Geochem. 15, 403–413.

Papacostas, N.C., Bostick, B.C., Quicksall, A.N., Landis, J.D., Sampson, M., 2008. Geomorphic controls on groundwater arsenic distribution in the Mekong River Delta, Cambodia. Geology 36, 891–894.

Passos, M.P., Soares, E.A.A., Tatumi, S.H., Yee, M., Mittani, J.C.R., Hayakawa, E.H., Salazar, C.A., 2020. Pleistocene-Holocene sedimentary deposits of the Solimões-Amazonas fluvial system, Western Amazonia. J. S. Am. Earth Sci. 98 (102455), 0895–9811. https://doi.org/10.1016/j.jsames.2019.102455.

Podgorski, J., Berg, M., 2020. Global threat of arsenic in groundwater. Science 368, 845–850. https://doi.org/10.1126/science.aba1510.

Polizzotto, M.L., Kocar, B.D., Benner, S.G., Sampson, M., Fendorf, S., 2008. Near-surface wetland sediments as a source of arsenic release to ground water in Asia. Nature 454, 505–508.

Postma, D., Larsen, F., Thai, N.T., Pham, T.K.T., Jakobsen, R., Nhan, P.Q., Long, T.V., Viet, P.H., Murray, A.S., 2012. Groundwater arsenic concentrations in Vietnam controlled by sediment age. Nat. Geosci. 5, 656–661.

Puhakka, M., Kalliola, R., Rajasilta, M., Salo, J., 1992. River types, site evolution and successional vegetation patterns in Peruvian Amazonia. J. Biogeogr. 19, 651–665.

Pupim, F.N., Sawakuchi, A.O., Almeida, R.P., Ribas, C.C., Kern, A.K., Hartmann, G.A., Chiessi, C.M., Tamura, L.N., Mineli, T.D., Savian, J.F., Grohmann, C.H., Bertassoli Jr., D.J., Stern, A.G., Cruz, F.W., Cracraft, J., 2019. Chronology of Terra firme formation in Amazonian lowlands reveals a dynamic Quaternary landscape. Quat. Sci. Rev. 210, 154–163.

Quicksall, A.N., Bostick, B.C., Sampson, M.L., 2008. Linking organic matter deposition and iron mineral transformations to groundwater arsenic levels in the Mekong delta, Cambodia. Appl. Geochem. 23, 3088–3098.

Quispesivana, Q.L., Zapata, M.A., Sánchez, I.J., Álvarez, C.D., Lagos, M.A., Atencio, A.E., Cuyubamba, P.V., 1999. Geología de los cuadrángulos 5-k, 5-l, 5-m, 6-h, 6-i, 6-j, 6-k, 6-l, 6-m, 7-k, 7-l, 7-m, 8-k, 8-l, 8-m, 9-j, 9-k, 9-l, 9-m, 10-j, 10-k, 10l y 10-m. INGEMMET, Boletín Serie A 130, 206.

Radloff, K.A., Zheng, Y., Stute, M., Weinman, B., Bostick, B., Mihajlov, I., Bounds, M., Rahman, M.M., Huq, M.R., Ahmed, K.M., Schlosser, P., van Geen, A., 2017. Reversible adsorption and flushing of arsenic in a shallow, Holocene aquifer of Bangladesh. Appl. Geochem. 77, 142–157.

Räsänen, M., Neller, R., Salo, J., Jungner, H., 1992. Recent and ancient fluvial deposition systems in the Amazonian foreland basin,Peru. Geol. Mag. 129, 293–306.

Räsänen, M.E., Salo, J.S., Jungner, H., Pittman, L.R., 1990. Evolution of the Western Amazon Lowland relief: impact of Andean foreland dynamics. Terr. Nova 2, 320–332.

Räsänen, M.E., Salo, J.S., Kalliola, R.J., 1987. Fluvial perturbance in the Western Amazon Basin – regulation by long-term sub-Andean tectonics. Science 238, 1398–1401.
Ravenscroft, P., Brammer, H., Richards, K.S., 2009. Arsenic Pollution: A Global Synthesis. Wiley-Blackwell, West Sussex (579 p).
Rebata-H, L.A., Korkka-Niemi, K., Heikkinen, P.-M., Räsänen, M.E., 2009. Hydrogeochemical characterisation of the Miocene Pebas and Nauta formations in Peruvian Amazonia. Bol. Soc. Geol. Perú 103, 125–151.
Roddaz, M., Viers, J., Brusset, S., Baby, P., Herail, G., 2005. Sediment provenances and drainage evolution of the Neogene Amazonian foreland basin. Earth Planet. Sci. Lett. 239, 57–78.
Rossetti, D.F., 2014. The role of tectonics in the late Quaternary evolution of Brazil's Amazonian landscape. Earth Sci. Rev. 139, 362–389.
Rossetti, D.F., Cohen, M.C.L., Bertani, T.C., Hayakawa, E.H., Paz, J.D.S., Castro, D.F., Friaes, Y., 2014. Late Quaternary fluvial terrace evolution in the main southern Amazonian tributary. Catena 116, 19–37.
Rozo, M.G., Nogueira, A.C.R., Truckenbrodt, W., 2012. The anastomosing pattern and the extensively distributed scroll bars in the middle Amazon River. Earth Surf. Process. Landf. 37, 1471–1488.
Ruokolainen, K., Moulatlet, G.M., Zuquim, G., Hoorn, C., Tuomisto, H., 2019. Geologically recent rearrangements in central Amazonian river network and their importance for the riverine barrier hypothesis. Front. Biogeogr. 11 (3). https://doi.org/10.21425/F5FBG45046.
Sioli, H., 1956. Über Natur und Mensch im brasilianischen Amazonasgebiet. Erdkunde 10 (2), 89–109.
Silva, C.L., Morales, M., Crósta, A.P., Costa, S.S., Jiménez-Rueda, J., 2007. Analysis of tectonic-controlled fluvial morphology and sedimentary processes of the western Amazon Basin: an approach using satellite images and digital elevation model. An. Acad. Bras. Cienc. 79 (4), 693–711.
Smedley, P.L., Kinniburgh, D.G., 2002. A review of the source, behavior and distribution of arsenic in natural waters. Appl. Geochem. 17, 517–568. https://doi.org/10.1016/S0883-2927(02)00018-5.
Smith, A.H., Lingas, E.O., Rahman, M., 2000. Contamination of drinking-water by arsenic in Bangladesh: a public health emergency. Bull. World Health Organ. 78 (9), 1093–1103.
Soares, E.A.A., Tatumi, S.H., Riccomini, C., 2010. OSL age determinations of Pleistocene fluvial deposits in Central Amazonia. An. Acad. Bras. Cienc. 82 (3), 691–699.
Stahl, M.O., Harvey, C.F., van Geen, A., Sun, J., Trang, P.T.K., Lan, V.M., Phuong, T.M., Viet, P.H., Bostick, B.C., 2016. River bank geomorphology controls groundwater arsenic concentrations in aquifers adjacent to the Red River,Hanoi Vietnam. Water Resour. Res. 52 (8), 6321–6334.
Stopelli, E., Duyen, V.T., Mai, Prommer H., Glodowska, M., Kappler, A., Schneider, M., Eiche, E., Lightfoot, A.K., Schubert, C.J., Trang, P.T.K., Viet, P.H., Kipfer, R., Winkel, L., Berg, M., AdvectAs team members, 2021. Carbon and methane cycling in arsenic-contaminated aquifers. Water Res. 200, 117300. https://doi.org/10.1016/j.watres.2021.117300.
Stuckey, J.W., Schaefer, M.V., Kocar, B.D., Benner, S.G., Fendorf, S., 2016. Arsenic release metabolically limited to permanently water-saturated soil in Mekong Delta. Nat. Geosci. 9, 70–76.
van Geen, A., Zheng, Y., Versteeg, R., Stute, M., Horneman, A., Dhar, R., Steckler, M., Gelman, A., Small, C., Ahsan, H., Graziano, J.H., Hussain, I., Ahmed, K.M., 2006. Spatial variability of arsenic in 6000 tube wells in a 25 km2 area of Bangladesh. Water Resour. Res. 39 (5), 1140. https://doi.org/10.1029/2002WR001617.
van Geen, A., Bostick, B.C., Thi Kim Trang, P., et al., 2013. Retardation of arsenic transport through a Pleistocene aquifer. Nature 501 (7466), 204–207. https://doi.org/10.1038/nature12444.
Vauchel, P., Santini, W., Guyot, J.L., Moquet, J.S., Martinez, J.M., Espinoza, J.C., Baby, P., Fuertes, O., Noriega, L., Puita, O., Sondag, F., Fraizy, P., Armijos, E., Cochonneau, G., Timouk, F., de Oliveira, E., Filizola, N., Molina, J., Ronchail, J., 2017. A reassessment of the suspended sediment load in the Madeira River basin from the Andes of Peru and Bolivia to the Amazon River in Brazil, based on 10 years of data from the HYBAM monitoring programme. J. Hydrol. 553, 35–48.
Wallis, I., Prommer, H., Berg, M., Siade, A.J., Sun, J., Kipfer, R., 2020. The river–groundwater interface as a hotspot for arsenic release. Nat. Geosci. 13 (4), 288–295.
Wasserman, G.A., Liu, X.H., Parvez, F., Ahsan, H., Levy, D., Factor-Litvak, P., Kline, J., van Geen, A., Slavkovich, V., Lolacono, N.J., Cheng, Z.Q., Zheng, Y., Graziano, J.H., 2006. Water manganese exposure and children's intellectual function in Araihazar, Bangladesh. Environ. Health Perspect. 114, 124–129.
Weinman, B., Goodbred, S.L., Zheng, Y., Aziz, Z., Steckler, M., van Geen, A., Singhvi, A.K., Nagar, Y.C., 2008. Contributions of floodplain stratigraphy and evolution to the spatial patterns of groundwater arsenic in Araihazar, Bangladesh. Geol. Soc. Am. Bull. 120, 1567–1580.
WHO, 2011. Guidelines for Drinking-water Quality. 4th ed. Geneva.
Winkel, L., Berg, M., Amini, M., Hug, S.J., Johnson, C.A., 2008. Predicting groundwater arsenic contamination in Southeast Asia from surface parameters. Nat. Geosci. 1, 536–542.
Winkel, L.H.E., Pham, T.K.T., Vi, M.L., Stengel, C., Amini, M., Nguyen, T.H., Pham, H.V., Berg, M., 2011. Arsenic pollution of groundwater in Vietnam exacerbated by deep aquifer exploitation for more than a century. Proc. Natl. Acad. Sci. U. S. A. 108, 1246–1251. https://doi.org/10.1073/pnas.1011915108.
Ying, S.C., Schaefer, M.V., Cock-Esteb, A., Li, J., Fendorf, S., 2017. Depth stratification leads to distinct zones of manganese and arsenic contaminated groundwater. Environ. Sci. Technol. 51, 8926–8932.
Zhang, Z., Guo, H., Liua, S., Weng, A., Han, S., Gao, Z., 2020. Mechanisms of groundwater arsenic variations induced by extraction in the western Hetao Basin, Inner Mongolia,China. J. Hydrol. 583, 124599. https://doi.org/10.1016/j.jhydrol.2020.124599.